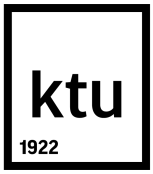

Kaunas University of Technology

Faculty of Electrical and Electronics Engineering

Efficient Methods for Electroencephalogram Signal Denoising

Master's Final Degree Project

Mohammad Shahbakhti

Project Author

Prof. Dr. Vaidotas Marozas

Supervisor

KAUNAS, 2020

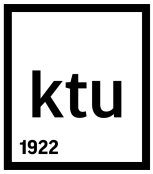

Kaunas University of Technology

Faculty of Electrical and Electronics Engineering

Efficient Methods for Electroencephalogram Signal Denoising

Master's Final Degree Project
Biomedical Engineering (6211EX002)

Mohammad Shahbakhti
Project Author

Prof. Dr. Vaidotas Marozas
Supervisor

Prof. Dr. Linas Svilainis
Reviewer

KAUNAS, 2020

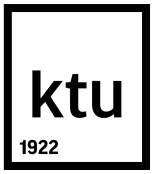

Kaunas University of Technology
Faculty of Electrical and Electronics Engineering
Mohammad Shahbakhti

Efficient Methods for Electroencephalogram Signal Denoising

Declaration of Academic Integrity

I confirm that the final project of mine, Mohammad Shahbakhti, on the topic „Efficient Methods for Electroencephalogram Signal Denoising“ is written completely by myself; all the provided data and research results are correct and have been obtained honestly. None of the parts of this thesis have been plagiarised from any printed, Internet-based or otherwise recorded sources. All direct and indirect quotations from external resources are indicated in the list of references. No monetary funds (unless required by Law) have been paid to anyone for any contribution to this project.

I fully and completely understand that any discovery of any manifestations/case/facts of dishonesty inevitably results in me incurring a penalty according to the procedure(s) effective at Kaunas University of Technology.

(Mohammad Shahbakhti) *(Signature)*

Shahbakhti, Mohammad. Efficient Methods for Electroencephalogram Signal Denoising. Master's Final Degree Project. / Supervisor Prof. Dr, Vaidotas Marozas; Faculty of Electrical and Electronics Engineering, Kaunas University of Technology.

Study field and area: Bioengineering, Engineering Science

Keywords: EEG, Artifacts, Eye blink, Electrical shift and linear trend, SWT, Skewness, Kurtosis.

Kaunas, 2020. 41.

Summary

Electroencephalography (EEG) is a non-invasive electrophysiological technique to record and monitor the electrical activity of the brain from electrodes placed along the scalp. In last two decades, a wide range applications of EEG signals have been proposed such as, not limit to, epilepsy detection and prediction, diagnosis of sleep disorders, depth of anesthesia and coma, Brain Computer Interfaces (BCI) applications, etc.

The utilization of recorded EEG signals might be hindered due to artifacts and noise of physiological and non-physiological sources, e.g., eye blinks (EB), eye movements, muscle contractions, cardiac activity, electrical shift and linear trend (ESLT), power line interference, etc. The influence of these artifacts might lead to the wrong statistical and physiological analysis of the brain activity. In particular for long-term EEG recordings or autonomous BCI systems, where the noise contribution is random and cannot be supervised by the human expert, the automatic elimination of EEG artifacts is a necessary step before further processing and analysis. Amongst artifacts with the physiological origin, EB, due to its large amplitude and inevitable frequent appearance, is considered to have the most adverse influence on the EEG analysis. ESLT artifacts may emerge in EEG signals due to the temporary shift or lose of electrodes during the recording.

In this thesis, low complexity approaches based on the Stationary Wavelet Transform (SWT) for the elimination of EB and ESLT artifacts from EEG signals are proposed. The main novelty of this research is to employ skewness and kurtosis to stop the decomposition level of SWT once it reaches the artifact components. It is shown that the skewness and kurtosis could be suitable artifact markers for EB and ESLT, respectively. The proposed methods are compared against the Automatic Wavelet Independent Components Analysis (AWICA) and Enhanced AWICA (EAWICA) which were presented for automatic EEG denoising. The performance of all algorithms have been tested on simulated and real contaminated EEG signals. Normalized Root Mean Square Error (NRMSE), Peak Signal-to-Noise Ratio (PSNR), and correlation coefficient (CC) between filtered and pure EEG signals are utilized to quantify artifact removal performance. The proposed approaches show smaller NRMSE and larger PSNR, and CC values compared to the other methods. Furthermore, the speed of execution for the proposed algorithms are considerably shorter than the algorithms for comparison, which makes them more suitable for the real-time processing.

Acknowledgments

This research is dedicated to care workers all around the world, who put their life in jeopardy to fight against Covid-19 outbreak and save other's life. I would like to express my deepest gratitude to my supervisor, Professor Vaidotas Marozas, who has the substance of a genius: he convincingly guided and encouraged me to be professional and do the right thing even when the road got tough. Without his persistent help, the goal of this project would not have been realized. I would like to pay my special regards to my family, my wife, Somayeh; my parents and sisters for their persistent and unconditional supports during the last two years. Last but not the least, I wish to thank Ana Rodrigues, Dr. Andrius Solosenko, Professor Piotr Augustyniak, Dr. Andrius Petrenas and Dr. Anna Broniec-Wojcik whose assistance was a milestone in the publications of this research.

Contents

Terms and Definitions

EEG - Electroencephalography
BCI - Brain Computer Interface
EB - Eye Blink
ESLT - Electrical Shift and Linear Trend
SWT - Stationary Wavelet Transform
AWICA - Automatic Wavelet Independent Components Analysis
EAWICA - Enhanced AWICA
NRMSE - Normalized Root Mean Square Error
PSNR - Peak Signal-to-Noise Ratio
CC - Correlation Coefficient
PSD - Power Spectral Density
MSC - Magnitude Squared Coherence

Introduction

Recording of the electrical activity from the surface of scalp is called Electroencephalography (EEG). It is a non-invasive technique which is also considered as the cheapest strategy to study the brain's activity. The most prominent advantage of EEG is the capability of observing the brain's scheme in real time with milliseconds resolution. Environmental flexibility to be used in indoors not only clinics, is another benefit of EEG compared to other techniques for studying the brain.

EEG signals recorded from the scalp are extensively used in the medical practice to analyze the brain activity for the diagnosis, the management and the investigation of neurological problems such as, but not limited to, epilepsy [1, 2], neurodegenerative diseases [3, 4] and sleep disorders [5, 6]. Another important application for the scalp EEG can be found in Brain Computer Interface (BCI), which has yielded significant advances in neurorehabilitation and assistive technologies, while also targeting the improvement of life's quality for disabled people [7]. BCI systems can substitute or refurbish purposeful function to people who deal with neurological disorders such as, not limit to, amyotrophic lateral sclerosis, cerebral palsy, stroke, or spinal cord injury. The emergence of low-cost electroencephalography (EEG) headbands with a few number of channels has yielded a significant leap in the healthcare monitoring and BCI systems. These recorded EEG signals are, however, corrupted by non-cerebral activity originating from physiological and non-physiological sources such as eye blink (EB), cardiac activity, muscle contraction, power line noise, electrical shift and linear trend (ESLT), etc. [8]. These sources distort the EEG signal and may affect the final detection or classification results. The artifact removal is, therefore, a critical and necessary step in the EEG signal processing.

In order to filter artifacts from EEG signals, a wide ranges of approaches have been proposed in literature. The main drawbacks of such methods are the necessity of an artifact channel recording for those based on adaptive filters, requirement of prior knowledge of the collected EEG signals for wiener filters and regression based methods, the lack of performance of linear filtering when the EEG signal and artifacts overlap in the same frequency band, the computational expensiveness of Blind Source Separation (BSS) methods, and the manual setting of the level of decomposition for source decomposition methods.

The aim of this work is to propose automatic algorithms for the filtering of artifacts from EEG signals.

The objectives of this research are as follow:

1. To develop low computational algorithms for eye blink, electrical shift and linear trend removal from EEG signal, without demanding the artifact reference or prior knowledge of the collected EEG signals.
2. To implement the proposed algorithms on simulated and real contaminated EEG signals.
3. To compare the performance and execution time of the proposed approaches with Automatic Wavelet Independent Component Analysis (AWICA) and Enhanced AWICA (EAWICA) algorithms.

1. Background

This chapter presents the background information regarding the generation of EEG signals in the brain, collecting EEG signals from the scalp, fluctuation of EEG rhythms, artifacts in EEG signals and literature review for the EEG denoising.

1.1. Physiology of EEG

There are billions of cells in the brain which half of them are neurons and half of them are to facilitate the neuron's activities. The neurons are tightly linked to synapses that operate as gateways of the inhibitory or excitatory activity. Any synaptic activity produces an elusive electrical pulse known as the postsynaptic potential. When thousands of the neurons act synchronously, an electrical filed is generated which is capable to be spread through skull and could be collected from the scalp which is known as EEG. In general terms, EEG signals are related to the discharge of thousands of nerve cells in the cortex (synaptic excitation), principally the pyramidal cells and their corresponding dendrites [9].

1.2. Acquisition of EEG

Collected EEG signals can be interpreted according to the four areas of the cortex (lobes): O-occipital lobe (primarily responsible for processing visual information), P-parietal lobe (primarily responsible for motor functions), T-temporal lobe (responsible for F-frontal lobe (basically responsible for executive functions) [10]. Fig 1.1 demonstrates the lobes of the brain.

According to this interpretation, Jasper [11] proposed 10/20 system to record EEG signals, which is the relationship between sites of the electrodes and the brain lobes. Numbers 10 and 20 are to specify the distance between the adjust electrodes which is either 10% or 20% of the whole front-back or right-left distance of the skull. Each electrode is named based on the lobe and hemisphere location. It should be noted that C-central lobe does not exist and is just to identify the purposes. Letter Z refers to the electrode place on the mid line. Even and odd numbers refer to the location of electrodes on the right and left hemisphere, respectively. Fig 1.2 shows the 10/20 international system to record EEG signals from the scalp.

The amplitude of the recorded EEG signals from scalp varies from 1 to 200 μvolts and the frequency range of them oscillates between 0.5 to 50 Hz. Brain oscillatory has been classified into five rhythms called Delta (0.5 to 3.5 Hz), which has the slowest oscillation with highest amplitude (up to 200 μVolts), Theta (3.5 to 7 Hz) which has relatively slow oscillation and high amplitude (up to 100 μvolts), Alpha (7 to 14 Hz) that has smaller amplitude then Theta but faster fluctuation, Beta (14 to 30 Hz) which has irregular small amplitude and Gamma (30 to 50 Hz) which has the fastest fluctuation. It should be noted the during an ongoing EEG signal, proportions of all rhythms might be included and these proportions can be changed in association with cognitive and sensory processes [9, 10]. Fig 1.3 shows an example of EEG signal and the corresponding rhythms.

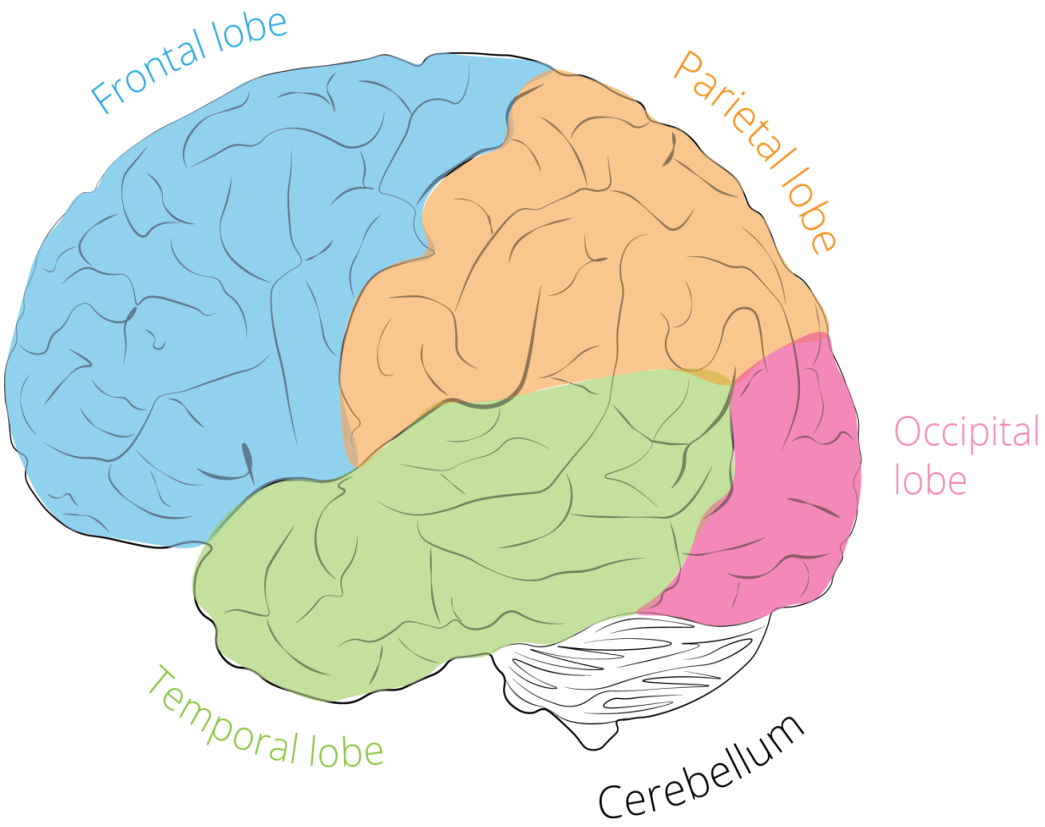

Figure 1.1 The lobes of the brain.

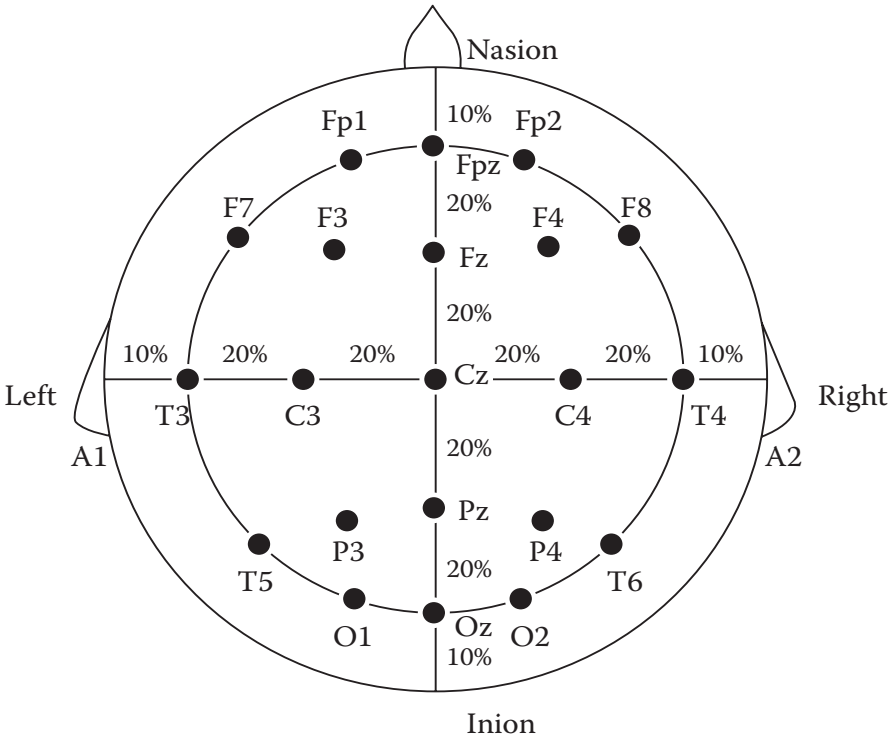

Figure 1.2 The location of EEG electrodes according to 10/20 system; adapted from [9].

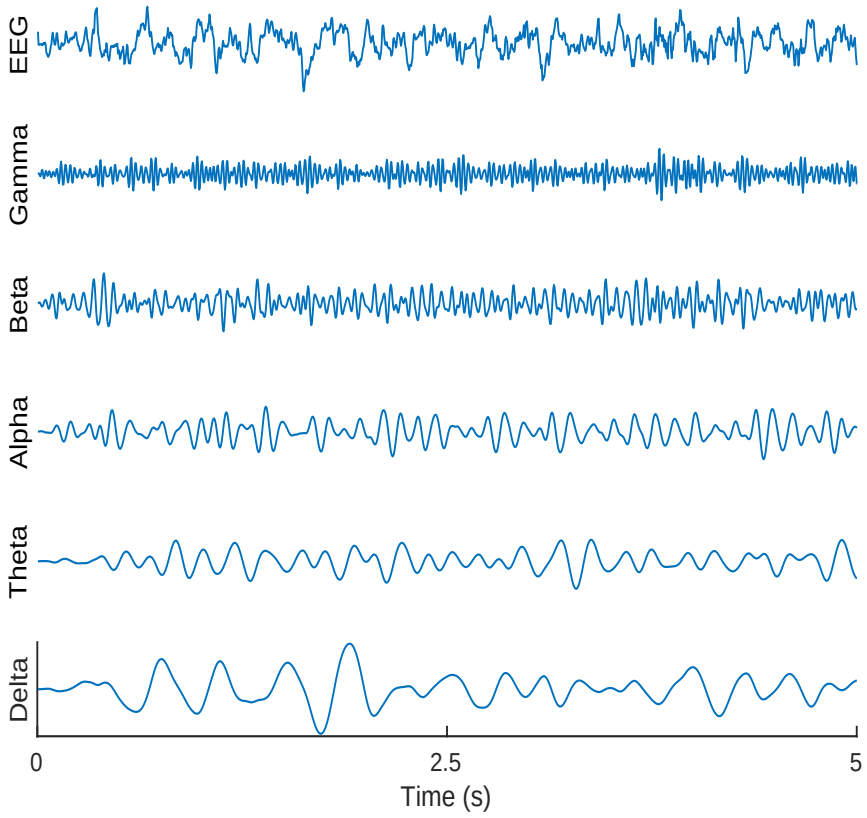

Figure 1.3 An EEG signal and the corresponding bands.

1.3. Artifacts in EEG signals

Unfortunately, EEG signals are extremely vulnerable to artifacts. According to the physiological literature, the artifacts in EEG signals might be categorized into those which has physiological sources such as EOG, ECG and EMG signals, and those which has non-physiological origins, for instance, power line noise and ESLT artifacts [8]. The influence of artifacts on EEG signals might be relatively proportional to the location of EEG channel and frequency range of the artifacts. For example, eye blink has a larger amplitude in frontal electrodes rather than temporal and it overlaps the Delta band of EEG, whereas, jaw muscle movement or verbalization has a stronger influence on temporal electrodes and overlaps the Beta band of EEG [9].

In this project, we just investigate the elimination of EB and ESLT artifacts from EEG signals.

Amongst physiological artifacts, eye blink is considered to have the most impact on the EEG signal analysis, due to its high amplitude and overlapping frequency components. The cornea (positive) and the retina (negative) of the human eye form an electrical dipole. Movements and blinks of the eye modify this dipole and generate an electrical signal known as EOG, inducing strong ocular artifacts in EEG recordings [12]. Eye blinks are characterized by low frequency components (<4 Hz) with a high amplitude which have a symmetrical activity mainly located on the front lobe electrodes with low propagation to other EEG channels. Eye movements are also identified as a low frequency signal (<4 Hz) with lower amplitude but higher propagation to other

electrode positions [13].

The occurrence of eye blinks is more frequent than eye movements, therefore, the elimination of eye blinks from EEG has gained more attention than the elimination of eye movements. Examples of clean and contaminated EEG signal with eye blinks is shown in Fig 1.4.

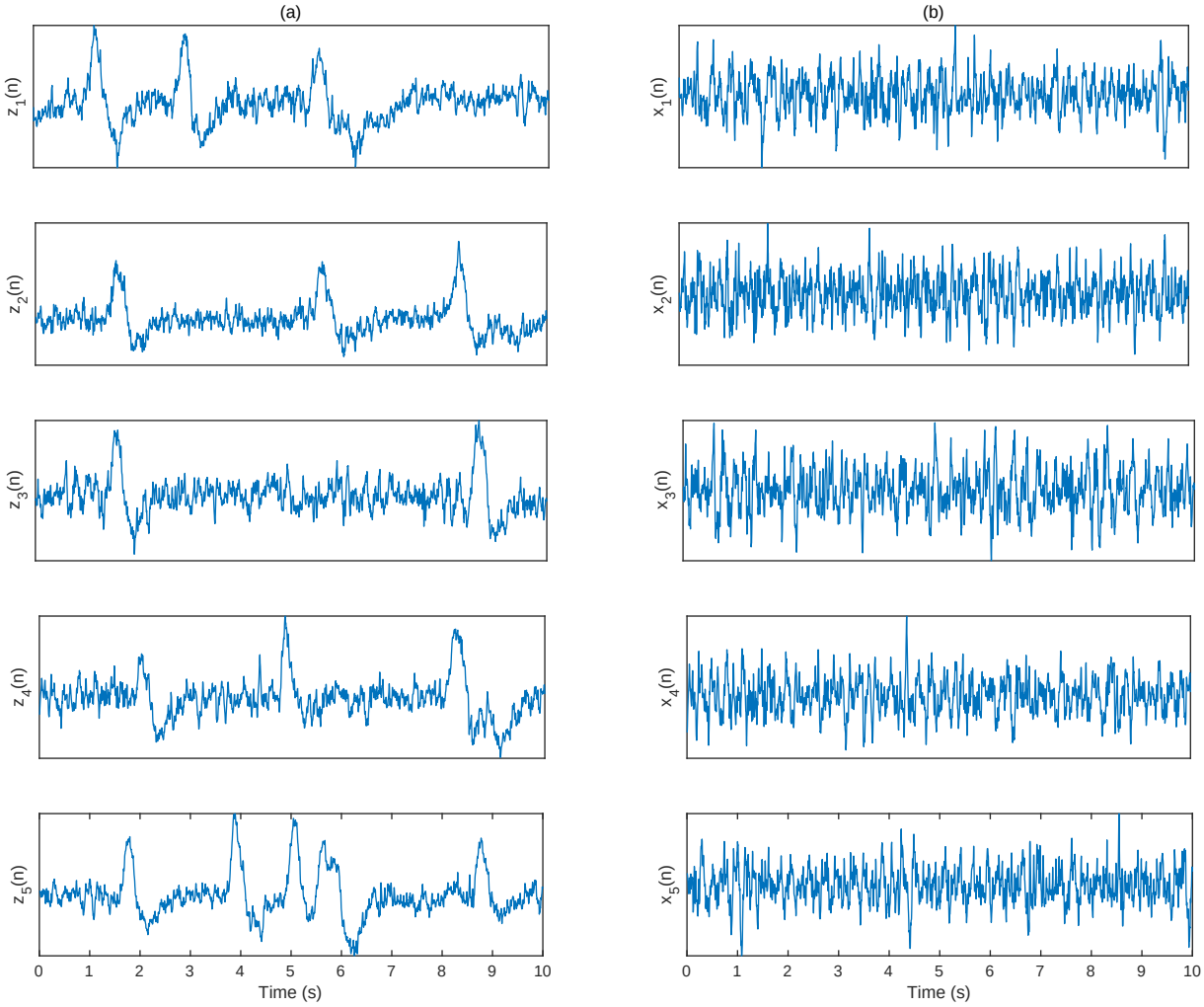

Figure 1.4 Examples of the contaminated (a) and the pure (b) EEG signals.

Unfortunately, the elimination of artifacts with non-physiological origin from EEG signals has not gained enough attention in the recent literature [14-16]. Apart form the power line interference, electrical shift (discontinuities) and linear trend could be considered as the most common artifacts with the non-physiological origin. The occurrence of ESLT artifact might be due to the electrode shifts or a temporary loss of the skin-electrode contact, transient recording-induced current drifts and electrical pop [17, 18]. Fig 1.5 illustrates examples of pure EEG and EEG contaminated to the ESLT artifact.

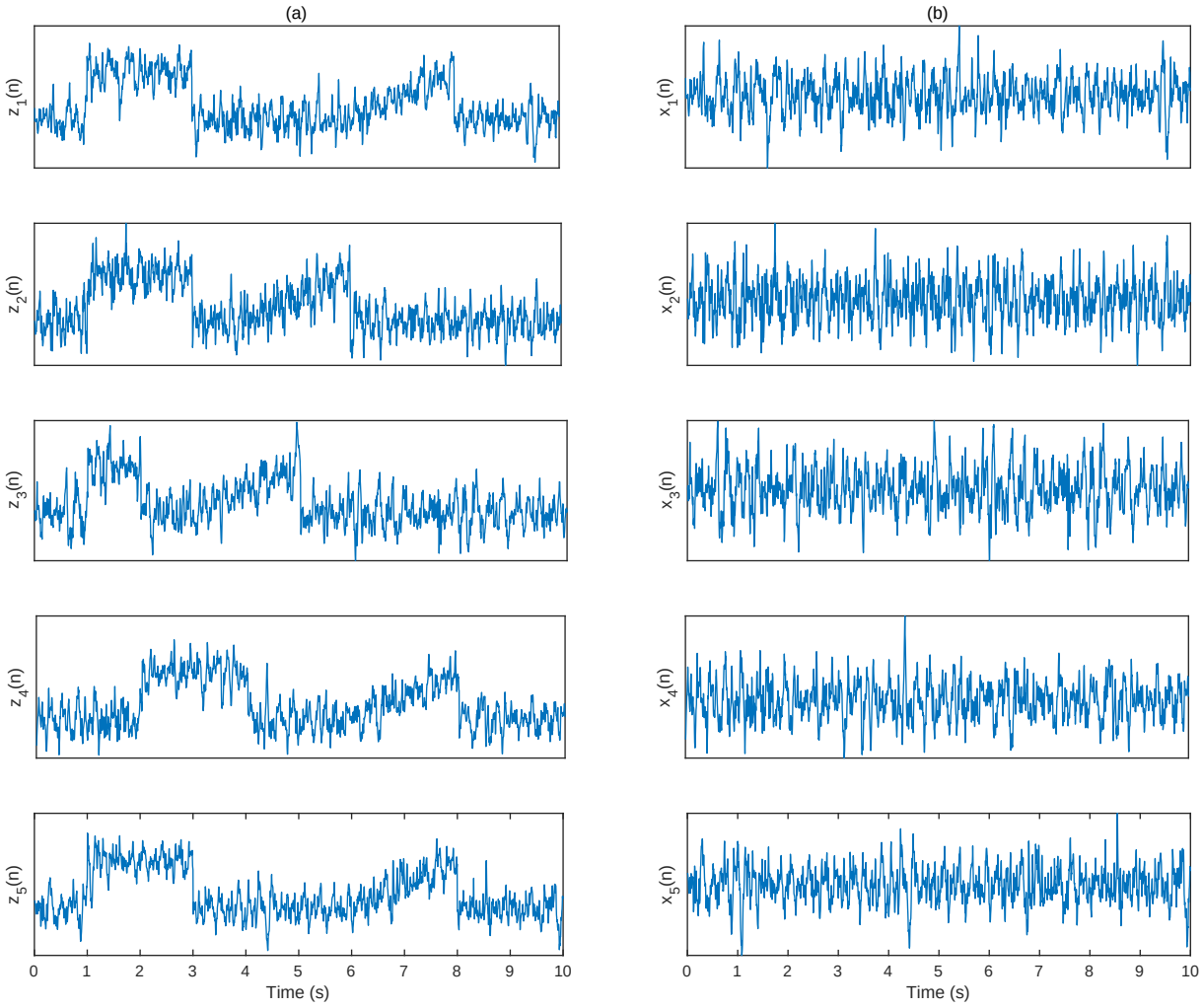

Figure 1.5 Examples of the contaminated (a) and the pure (b) EEG signals.

1.4. Analysis of EEG denoising methods

In order to have clean EEG signals, three main strategies can be considered. First of all, we can ignore all EEG segments which are contaminated to the artifacts and just use the free-of-artifact segments. Using such a strategy yield the loss of EEG of interest and might not leave enough data for further analysis. Second strategy is to ask subjects not generate any artifacts, however, the generation of some of artifacts such as eye blinks and cardiac activity are spontaneous. The third strategy is to filter the noisy artifacts while maintaining the EEG component for the segment of EEG that is filtered [19].

Obviously, the third strategy seems more effective, thus, an extensive range of methods have been employed based on this methodology. In this section, a comprehensive discussion over the most common methods for the EEG filtering is presented.

To remove artifacts from EEG signals, a wide range of techniques have been used such as, not limit to, linear and adaptive filters, Blind Source Separation (BSS) and Source decomposition

algorithms.

Linear filters are widely applied for EEG filtering in clinical practices, however, suppression of the artifact components without affecting the representation of underlying cognitive brain process is not possible, e.g, language [20] and decision making [21], thus, it cannot be a reliable approach for neuroscience applications.

Conventional adaptive filters are considered as the most common method for the on-line removal of the artifacts from EEG signals [22]. Nevertheless, the recording of artifact reference might increase the complexity for wearable applications, e.g., long-term EEG monitoring [23, 24]. Additionally, the recording of the reference pattern of some artifacts such as the electrical shift and linear trend is unfeasible.

In order to overcome the requirement of an extra channel to record the artifact reference, Wiener filters have been proposed to de-noise EEG signals [25, 26]. The goal of Wiener filter is to minimize the Mean Square Error (MSE) between the desired and estimated signals. To this aim, estimation of power spectral densities (PSD) between the signal and the artifact is used. Despite this method does not need to the artifact reference, initial calibration is necessary.

Blind Source Separation (BSS) algorithms have gained lots of attentions for the EEG signals pre-processing as they do not require the reference artifact and prior knowledge of the collected EEG signals[27]. BSS approaches identify equivalent principal or independent components of the EEG signals and then apply the processing in the transformed domain. The most popular BSS algorithms for EEG signal processing are Principal Component Analysis (PCA) and Independent Component Analysis (ICA). Some studies suggested that PCA fails when EEG signals and the corresponding artifacts have the resembling amplitude [28, 29]. The assumption of ICA is based on the statistical independence of the EEG signals and the artifact sources, as a result, large number of data are required to achieve reliable results [22]. The other drawback of ICA is high computational demand [25].

Source decomposition algorithms have been widely employed for the artifact reduction in EEG signals, e.g, Empirical Mode Decomposition (EMD) [30, 31], Variational Mode Decomposition (VMD) [32 ,33] and Wavelet Transforms (WT) [34–37].

EMD has been recognized as a suitable method to analyze nonlinear and non-stationary signals. As a result, it has been widely employed for the EEG signal preprocessing. The aim of EMD is to decompose a signal into series of basis functions called Intrinsic Mode Functions (IMF), and one residue [38]. The main drawback of EMD is its poor robustness to noise as its performance might be influenced by white noise. To overcome this limitation, Ensemble EMD [39] and VMD [32 ,33] methods have been introduced, however, as a cost of the significant increase of the computational complexity.

Discrete Wavelet Transform (DWT) and Stationary Wavelet Transform (SWT) have been widely applied for EEG signal processing. The critical disadvantage of DWT lies in its time-variance property, which yields the number of coefficients decreasing by a factor 2 for each level of decomposition. SWT overcomes translation-variance of DWT by upsampling the components instead of downsampling. As a result, SWT components have the same length as the original signal [19].

Some studies suggested that SWT is more effective for the preprocessing of EEG signals since it provides better time resolution for the artifact characterization, as well as a smoother estimation of the EEG signal after the thresholding in the wavelet domain [40, 41].

Recently, hybrid algorithms based on BSS and source decomposition methods has received a lot of attention for the EEG signal pre-processing [17, 42-44]. Despite the adequate performance of these algorithms for EEG denoising, the computational time is still a problem.

Nadia et al [17, 42] presented two fully automatic algorithms based on the wavelet transform and ICA for the elimination of the eye blink, EMG, electrical shift and linear trend artifacts from EEG signals, called Automatic Wavelet Independent Component Analysis (AWICA) and Enhanced AWICA (EAWICA). Despite the fully automatic operation, the performance of these methods relies on the accurate setting of five parameters before the processing. Table 1.1 shows the information about different methods.

Table 1.1. Comparison of Different Methods for EEG Denoising

Method	Reference Electrode	Prior Knowledge	Computational Complexity	Online	Auto	Channel Setting	Denoising Quality
Linear Filter	No	No	Low	Yes	Yes	Single	Low
Wiener Filter	No	Yes	High	No	Yes/No	Single	High
Adaptive Filters	Yes	No	Low	Yes	Yes	Single	High
Linear Regression	Yes	Yes	Low	Yes	No	Single/Multi	Intermediate
ICA	No	No	High	No	Yes/No	Multi	High
PCA	No	No	Intermediate	No	Yes/No	Single/Multi	Intermediate
EMD	No	No	Low	Yes/No	Yes/No	Single/Multi	Intermediate
EEMD	No	No	Intermediate	Yes/No	Yes/No	Single/Multi	High
VMD	No	No	High	No	Yes/No	Single	High
WT	No	No	Low	Yes	Yes	Single/Multi	High
Hybrid Algorithms	No	No	High	No	Yes	Single/Multi	High

2. Materials and Methods

In this chapter, the proposed methods for the elimination of EB and ESLT artifacts from EEG signals using SWT, algorithms for comparison, the procedure of simulated data generation, real data and performance metrics are described.

2.1. Stationary Wavelet Transform

Discrete Wavelet Transform (DWT) have been extensively employed for biomedical researches as it represents a signal in both time and frequency domains, synchronously. Let $x(n)$ be a signal with N number of samples. DWT decomposes $x(n)$ into low and high frequency components called approximation components $a(n)$ and detail components $d(n)$ by passing it through a series of the filter banks. To this end, $x(n)$ is filtered by a low-pass filter $G(n)$ and high-pass filter $H(n)$ which gives $a_1(n)$ and $d_1(n)$ with $N/2$ samples. This procedure continues over approximation components by increasing number of decomposition level. Fig2.1 shows the DWT block diagram.

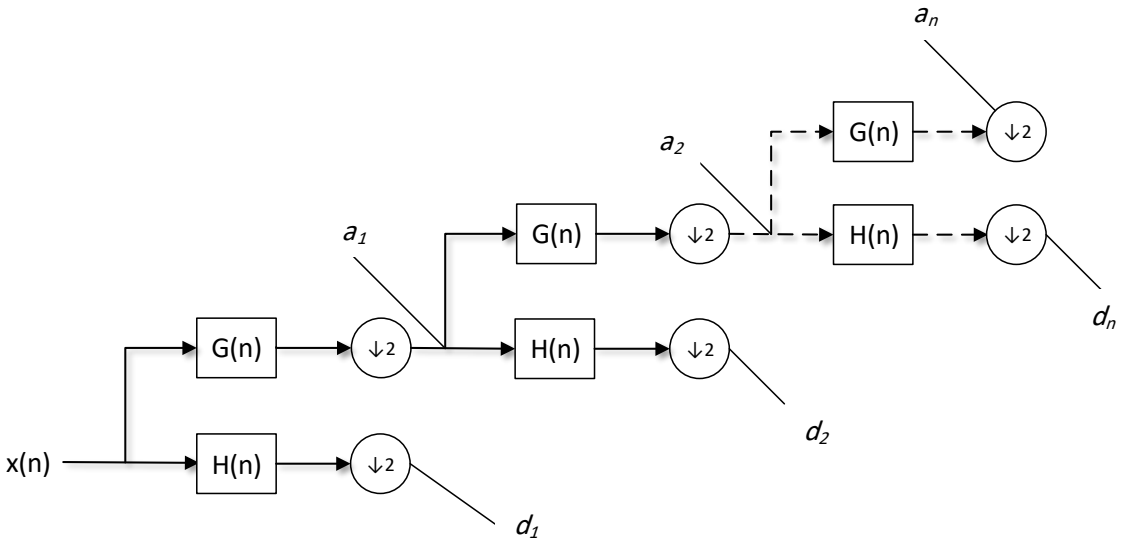

Figure 2.1 Block diagram of DWT algorithms.

The main disadvantage of DWT algorithm is its translational variant property which is resulted from the decimation operators with factor of two at each level. In order to over come this problem, SWT algorithm has been proposed. SWT solves translation-invariance of DWT, which is achieved by removing down-samplers. As a result, the approximation and detail components of SWT contain at each level have the same number of the samples as the original signal. Compared to DWT, SWT can achieve a better resolution by a factor of two up-sampling the components of the low pass and high pass filters at each level of decomposition. Redundant property of SWT makes it more suitable algorithm for signal de-noising. Fig2.2 shows the SWT block diagram.

Two parameters are required to be determined before conventional SWT processing: the mother wavelet and the number of decomposition levels. The selection of the mother wavelet is generally based on similarities between the mother wavelet and the desired signal.

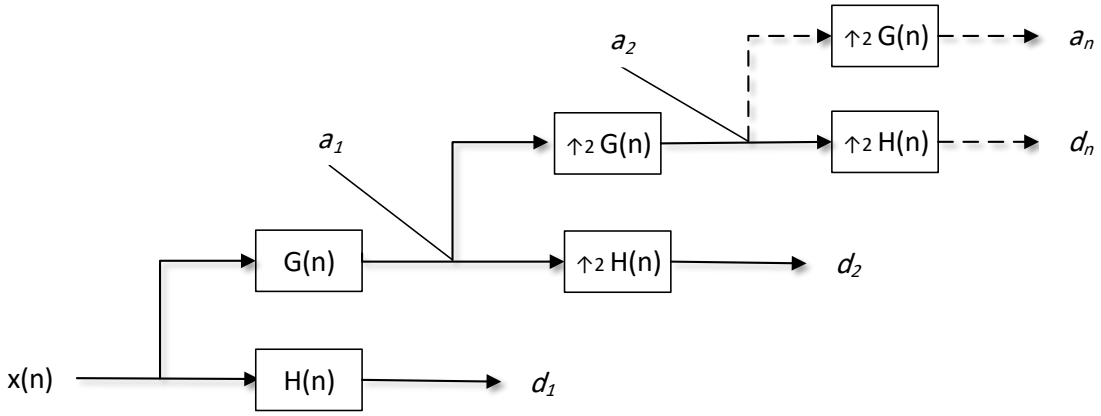

Figure 2.2 Block diagram of SWT algorithms.

The regulation of the decomposition level to reach artifact components for SWT is directly proportional to the sampling frequency of the recorded EEG signals. Hence, it may be changed for EEG signals sampled at different rates. In this thesis, new strategies which are independent of sampling frequency, for the automatic termination of SWT decomposition process when it achieves the artifact components are presented. As a result, the further decomposition is not required which may speed up the execution of the SWT filtering.

2.1.1. Proposed method for eye blink elimination

Daubechies wavelet 'db4' is commonly used as the mother wavelet for EEG signal processing [19, 40, 42, 44] as its morphology resembles eye blink signal. The spectrum of eye blink artifact varies between 0.01 to 3 Hz [13 ,19, 40]. Therefore, it is expected to increase the power of the frequencies in the lower end of the EEG spectrum, and as a result, the eye blink components lie in the last several levels of the SWT.

Since blinking is a low frequency phenomenon, it is expected to appear in approximation coefficients of SWT. Hence, the proposed criterion should be enforced on those coefficients. The presence of eye blinks may be indicated by a higher absolute value of skewness as it has a considerably larger amplitude compared to uncontaminated EEG signal [45, 46]. Fig 2.3 illustrates the examples of the signals and their histograms for pure EEG, blink artifact and blink contaminated EEG signal.

Skewness, S, for the signal x is defined as follows:

$$S = m_3 - 3m_2^2, \tag{2.1}$$

$$m_n = E\left[(x-\bar{x})^n\right], \tag{2.2}$$

where m_n indicates n^{th} order central moment of the variable. E and $\bar{x}$ are the expectation function and the mean of the signal, respectively.

For automatic stoppage of SWT when it reaches the blink artifact components, we have applied

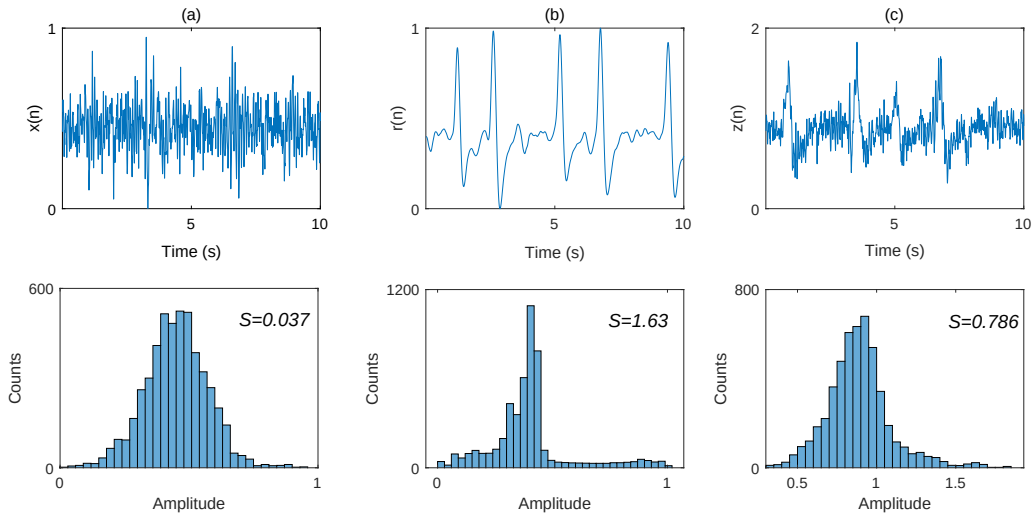

Figure 2.3 Examples of signals and histograms for clean EEG (a), blink artifact (b) and contaminated EEG (c). S is the skewness value.

a criterion based on the absolute difference of the absolute skewness values of two consecutive approximation coefficients levels. The block diagram of the proposed algorithm is shown in Fig 2.4.

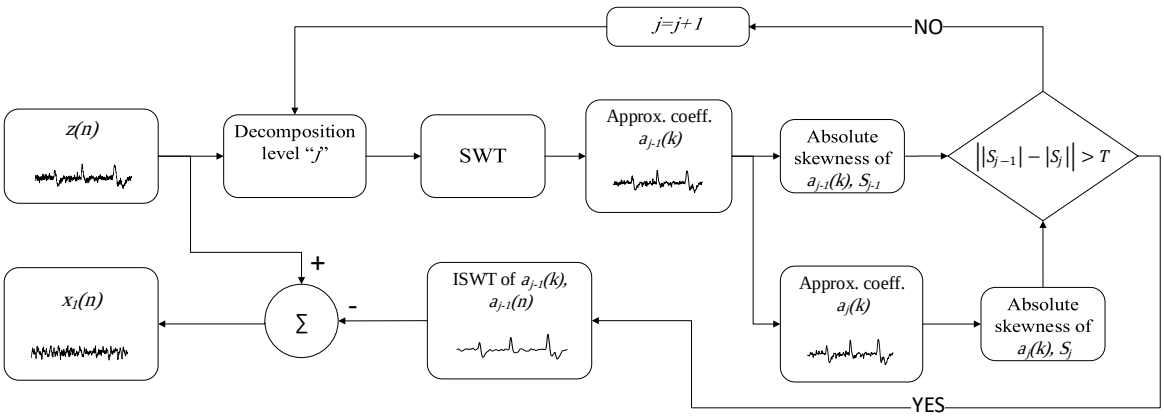

Figure 2.4 The block diagram of the proposed method for elimination of eye blinks from EEG signals.

The proposed criterion is defined as absolute difference of absolute skewness values of two consecutive approximation coefficients in SWT domain, which is expressed as follows:

$$\delta = \big||S_j| - |S_{j-1}|\big|, \tag{2.3}$$

where S is the skewness and j is the level of decomposition of SWT. If $\delta > T$, we can assume that SWT has reached the blink components. The approach to extract and remove eye blink components from the contaminated EEG is presented as follows:

1. Apply j level SWT to EEG signal contaminated with eye blinks, $z(n)$, and extract the approximation $a_{j-1}(n)$ and $a_j(n)$ coefficients, where $j = 2,3,...,J$ (wavelet domain).
2. Compute the absolute difference of absolute skewness values of $a_{j-1}(n)$ and $a_j(n)$ as δ.

3. If $\delta > T$, inverse SWT ($ISWT$) of $a_{j-1}(n)$ in order to get $a_{j-1}(n)$ which is considered as the eye blink artifact. Subtract $a_{j-1}(n)$ from the contaminated EEG signal $z(n)$ to obtain the filtered EEG signal. Otherwise, go back to step 1 and proceed to $j = j+1$.

In this paper, six T values ranging from 0.05 to 0.3 with a step of 0.05 have been applied. The optimal value of T was selected based on lowest mean of error between pure and filtered EEG signals.

2.1.2. Proposed method for electrical shift and linear trend elimination

Despite EB, ESLT artifacts consist of both low and high frequency components, thus, the appearance of these artifacts can be observed in both detail and approximation coefficients levels (Fig 2.5.

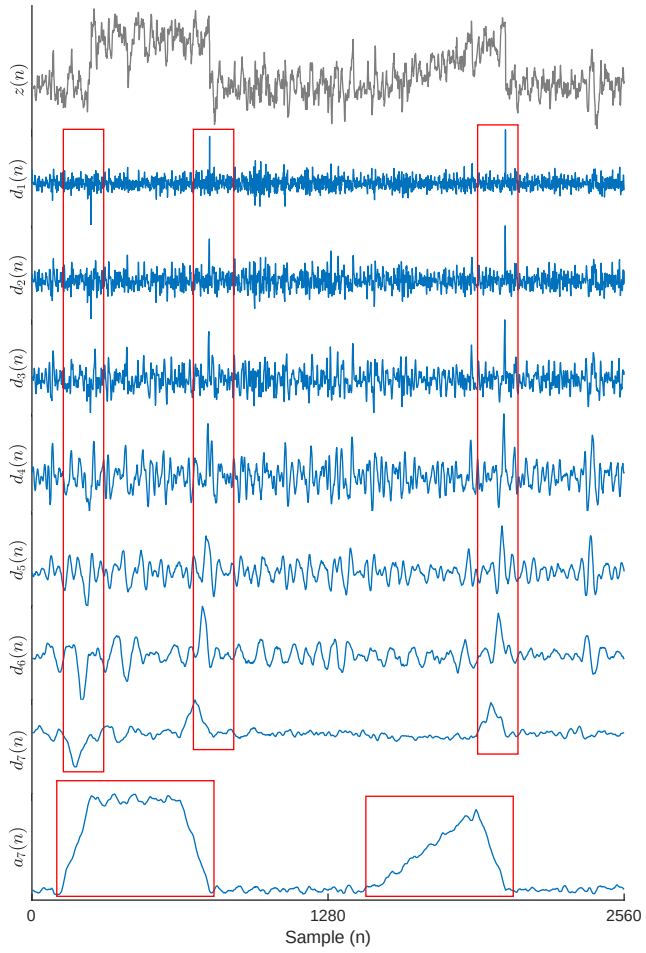

Figure 2.5 An example of the decomposed contaminated EEG signal.

Several studies showed that kurtosis may be applied as the criterion to detect artifacts in EEG signals [17, 18, 47-50]. The kurtosis is usually indicated by a high negative value due to either consistent sample values or the abrupt alteration of them between extremes. As EEG signals are quite dynamic, such activities cannot represent brain schemes. Therefore, it can be expected that the ESLT artifacts in EEG signals be indicated by the flat distribution with negative kurtosis [17, 48].

According to this discourse, we use the kurtosis to select the certain approximation coefficients level to remove low frequency components of ESLT and then filter the obtained detail coefficients levels to denoise high frequency components of ESLT artifact, to reconstruct EEG signals.

Kurtosis of the signal x is defined as follows:

$$k = m_4 - 3m_2^2, \tag{2.4}$$

$$m_n = E\left[(x-\bar{x})^n\right], \tag{2.5}$$

where m_n indicates n^{th} order central moment of the variable. E and $\bar{x}$ are the expectation function and the mean of the signal, respectively.

In order to stop the SWT decomposition process, the threshold is expressed based on the absolute difference of the kurtosis values calculated for approximation coefficients of two consecutive levels as follows:

$$\lambda = \left|K_j - K_{j-1}\right|, \tag{2.6}$$

where K is the kurtosis and j is the level of decomposition of SWT.

Filtering of the detail components is performed based on the following threshold [50]:

$$d_\theta(n) = \begin{cases} d(n) & \text{if } |d(n)| \leq \theta \\ 0 & \text{otherwise} \end{cases}, \tag{2.7}$$

$$\theta = \frac{\text{median}(|l|)}{0.6745}\sqrt{2\text{Log}N} \tag{2.8}$$

where $d(n)$ is the detail component and N is the signal length in samples.

Fig 2.6 shows the examples of clean and contaminated EEG signals, and the corresponding distributions.

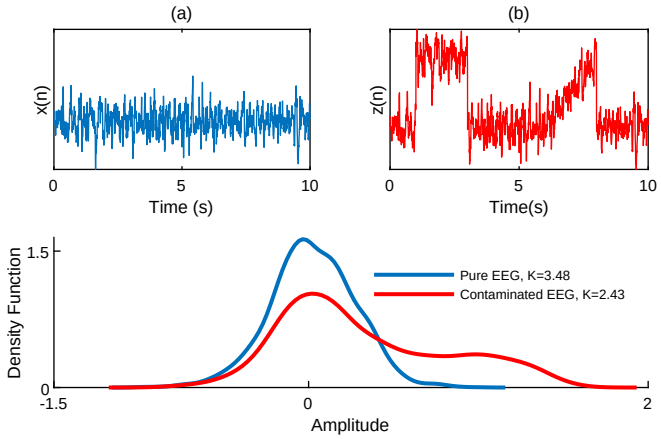

Figure 2.6 Examples of pure EEG (a), contaminated EEG (b) and the corresponding distributions (c). K is the kurtosis value.

The block diagram of the proposed method is shown in Fig 2.7.

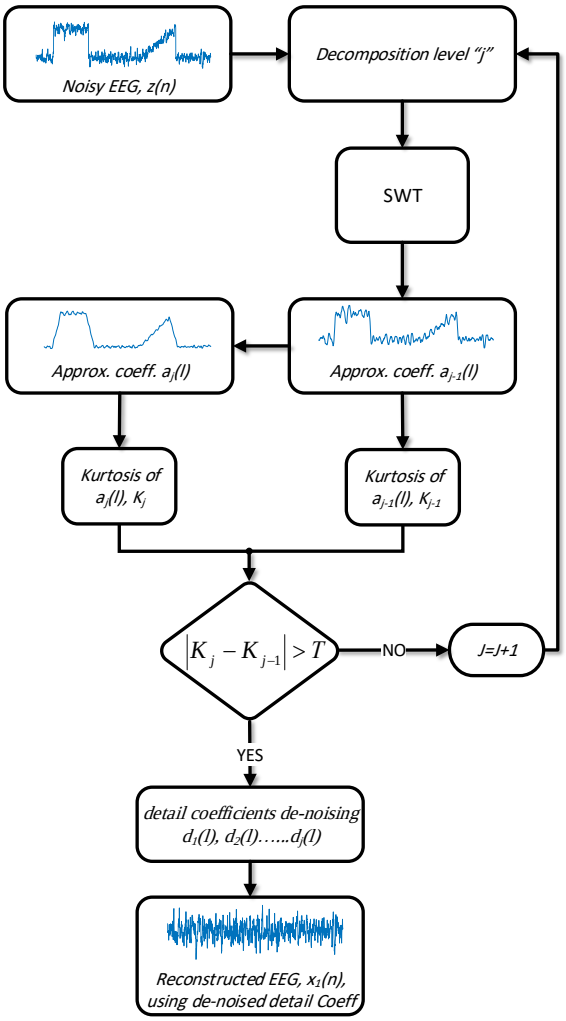

Figure 2.7 The block diagram of the proposed method for elimination of ESLT artifacts from EEG signals.

If $\lambda > T$, it is assumed that SWT has reached the optimal decomposition level for filtering of the ESLT artifacts. The following procedure has been applied to eliminate ESLT artifacts from EEG signals:

1. Apply j level SWT to the contaminated EEG signal, $z(n)$, and extract the approximation $a_{j-1}(n)$ and $a_j(n)$ coefficients, where $j = 2,3,...,J$ (wavelet domain).
2. Compute the absolute difference of the kurtosis values of $a_{j-1}(n)$ and $a_j(n)$ as λ.
3. If $\lambda > T$, denoise all extracted detail coefficients levels based on equation (2.7) and (2.8) and reconstruct the filtered EEG signal by $(ISWT)$. Otherwise, go back to step 1 and proceed with $j = j+1$.

In order to achieve the optimal threshold value, four values ranged from 0.05 to 0.2 with step value of 0.05 have been applied. The optimal threshold value is selected based on lowest mean of the error between the pure and the filtered EEG signals.

2.2. Algorithms for comparison

The performance of the proposed algorithms is compared with AWICA and EAWICA algorithms which are available from the authors upon request. The principle of these algorithms are based on joint of DWT and ICA, where DWT decomposes the EEG signal into its rhythms and then ICA is applied for the denoising. The main idea of these algorithms is to apply a two-step procedure relying on the concepts of kurtosis and Renyi's entropy to detect and eliminate artifacts from EEG signals. More details about these algorithms can be found in [17, 42]. There are five parameters required to be set before processing for AWICA and EAWICA algorithms. Optimal parameters were set as described in [42]. Fig 2.8 shows the block diagram of the algorithms for comparison.

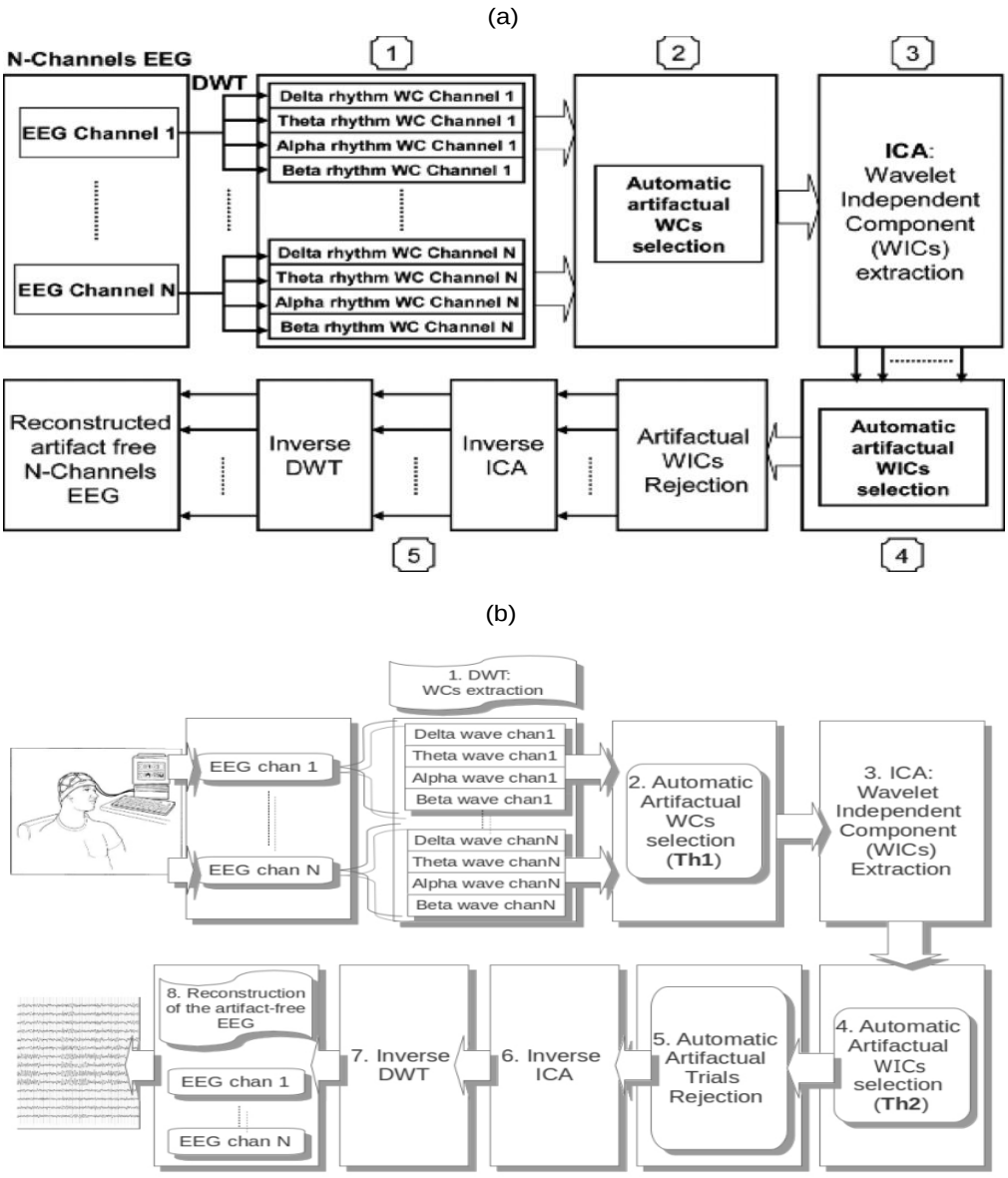

Figure 2.8 Block diagram of Algorithms for comparison. AWICA (a) adapted from [17] and EAWICA (b) adapted from [42].

2.3. Data

2.3.1. Generation of simulated data

Simulated EEG signals contaminated with artifacts are generated by an additive model as follows:

$$z(n) = x(n) + ar(n), \tag{2.9}$$

where $z(n)$ is the EEG signal contaminated with the artifact, $x(n)$ is the pure EEG and $r(n)$ is the artifact. Since propagation of artifacts is not equal in different lobes of the brain, the term a with four different values is applied to put emphasis on this fact that artifact magnitude is not equally distributed for all EEG channels [51].

2.3.2. Simulated data for EEG contaminated to eye blinks

Twenty four EEG signals from the CHB-MIT Scalp EEG database [52] (sampling rate Fs=256 Hz) have been selected to develop the proposed algorithm. We manually cut out 10 s long artifact-free EEG epochs, and in this way, we were able to collect pure EEG signals. 30 EEG signals collected during mental arithmetic tasks (EEG-MAT) (Fs = 500 Hz) [53] have been selected to test the performance of the proposed algorithm. EEG-MAT database had already been filtered and the data was clean. To generate simulated EEG signals contaminated with eye blinks, 54 real eye blink signals from the BCI experiment for motor imagery movement of the left and right hand [54], and the BCI Competition 2008 (Graz Data Sets 2a) [55] have been used. The eye blink signals were band-pass filtered between 0.1 and 3 Hz and resampled to 256 and 500 Hz. Therefore, the developing set of the algorithm includes a total of 24*4=96 and test set contains 30*4=120 of simulated signals. Fig 2.9 demonstrates examples of pure EEG, eye blink artifact, and blink contaminated EEG signals with different values of a for CHB-MIT database.

2.3.3. Simulated data for EEG contaminated to electrical shift and linear trend

In order to produce simulated EEG signals contaminated to the ESLT artifact, pure EEG signals from CHB-MIT database [52] have been added to twenty-four triangular and rectangular waves with four different bandwidths and amplitudes. Thus, 96 simulated data have been generated. Fig 2.10 shows examples of the contaminated EEG signals with different amplitudes.

2.3.4. Real data for EEG contaminated to eye blink

In order to assess the performance of the proposed method on real EEG signals contaminated with eye blinks, 8 EEG signals from the BCI experiment for motor imagery movement of the left and right hand ($fs = 512Hz$) [54] and 8 EEG signals from the BCI Competition 2008 (Graz Data Sets 2a) ($fs = 250Hz$) [55] with length of 60 seconds have been used. Each signal was divided into 6 windows of 10 seconds and then the denoising methods were applied. An eye blink reference channel was recorded simultaneously to EEG data for both databases. All raw EEG signals were

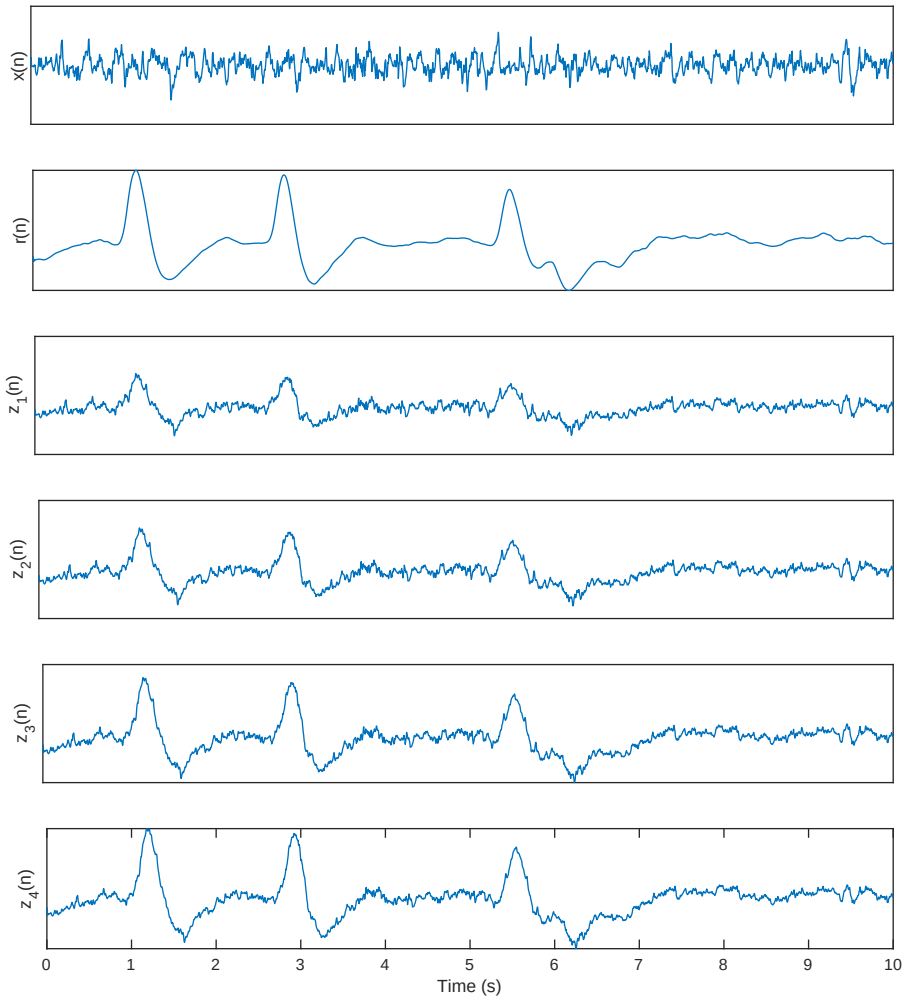

Figure 2.9 Examples of simulated data from CHB-MIT database. Pure EEG $x(n)$, eye blink artifact $r(n)$, contaminated EEG $z_1(n)$ - $a = 0.75$, $z_2(n)$ - $a = 1.0$, $z_3(n)$ - $a = 1.5$, and $z_4(n)$ - $a = 2.0$.

band pass filtered between 0.01 to 40 Hz and then the algorithms were performed to denoise the EEG signals.

2.3.5. Real data for EEG contaminated to electrical shift and linear trend

In order to assess the performance of the proposed method on real contaminated EEG signals, EEG-LAB [56] database that contains several artifacts has been applied. The signals were sampled at 128 Hz with length of 238 seconds. We manually selected epochs which contain ESLT artifacts to test the efficiency of the proposed method.

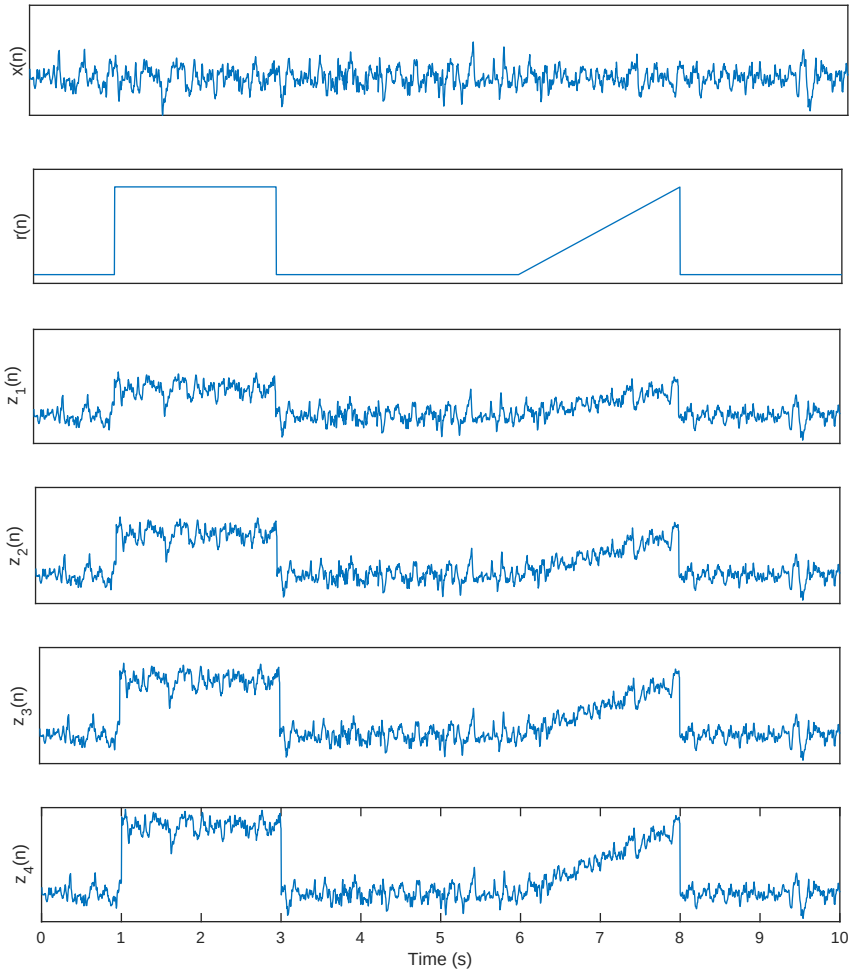

Figure 2.10 Examples of simulated data from CHB-MIT database: pure EEG $x(n)$, artificial ESLT artifact $r(n)$, contaminated EEG $z_1(n)$ - $a = 0.75$, $z_2(n)$ - $a = 1.0$, $z_3(n)$ - $a = 1.5$, and $z_4(n)$ - $a = 2.0$.

2.4. Denoising performance criteria

Normalized root mean square error $(NRMSE)$, peak signal-to-noise ratio $(PSNR)$ and correlation coefficient (ρ) between pure and filtered EEG signals are the principal performance measures in time domain. NRMSE and PSNR evaluate the magnitude distortion and ρ investigates phase distortion of the filtered EEG signals, respectively. NRMSE is defined as follows:

$$\text{NRMSE} = \frac{\sqrt{\frac{1}{N}\sum_{i=1}^{N}\left(x(n) - x_1(n)\right)^2}}{\max_{x(n)} - \min_{x(n)}} \times 100, \tag{2.10}$$

where $x(n)$ is pure EEG signal and $x_1(n)$ is filtered EEG signal.

PSNR is the peak error measurement which is expressed in decibels [40]:

$$\text{PSNR} = 20\log_{10}\left(\frac{\max_{x(n)}}{\sqrt{\frac{1}{N}\sum_{i=1}^{N}\left(x(n)-x_1(n)\right)^2}}\right). \tag{2.11}$$

Correlation coefficient is a value between 0 to 1 which is expressed as:

$$\rho = \frac{cov(x(n),x_1(n))}{\sigma_x(n)\sigma_{x_1}(n)}, \tag{2.12}$$

where *cov* is covariance and σ is standard deviation.

The algorithms have been executed on a computer with 3.2 GHz core i7 CPU, 16 GB RAM and with widely used computing software MATLAB R2018a (Mathworks Inc., Natick, Massachusetts, USA).

3. Results

3.1. Results for eye blink elimination

Fig 3.1 shows the Mean±SD of NRMSE between pure and filtered EEG signals per different values of T for CHB-MIT database. As observed below, the T value of 0.15, has the lowest NRMSE.

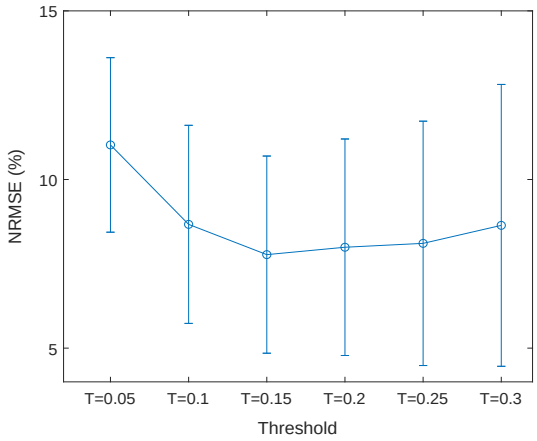

Figure 3.1 Mean±SD of NRMSEs per different T values.

Fig 3.2 shows an example of a decomposed contaminated EEG signal into approximation coefficients from CHB-MIT database in SWT domain. According to the proposed method, inverse SWT of $a_5(k)$ is considered as the eye blink artifact and is removed from the contaminated EEG.

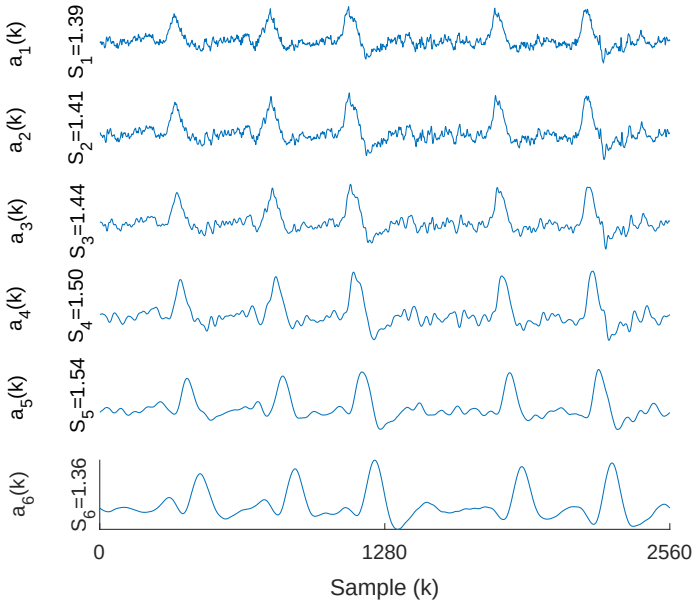

Figure 3.2 Examples of approximation coefficients and corresponding skewness values for a contaminated EEG signal from CHB-MIT database in SWT domain.

Quantitative analysis, computation of NRMSE, PSNR and correlation coefficient between pure and filtered EEG signals were solely performed for simulated data. For real EEG signals contaminated with eye blinks, performances are evaluated visually. Fig 3.3 illustrates the box plots of

NRMSE and correlation coefficient values between pure and filtered EEG signals for different databases and algorithms. The obtained results show that proposed algorithm, on average, performed better than the algorithms for comparison,

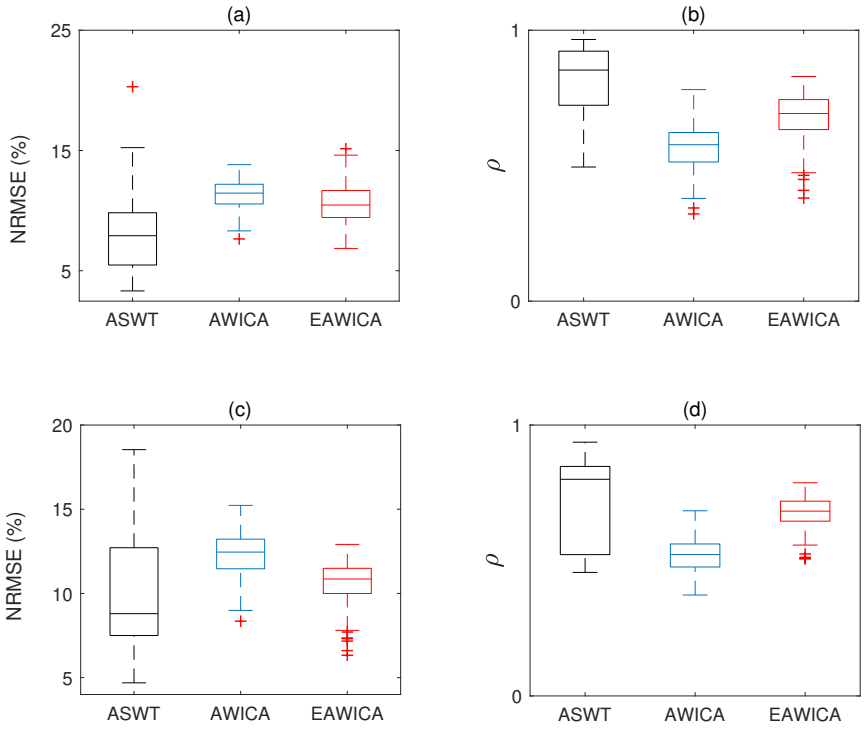

Figure 3.3 Box plots of NRMSE and correlation coefficient between pure and filtered EEG for simulated data by all methods. (a) and (b) are for CHB-MIT, (c) and (d) are for EEG-MAT databases.

Fig 3.4 shows examples of the contaminated, pure, and filtered EEG signals from both databases with all methods. while AWICA and EAWICA modified some clean segments of EEG, proposed method could preserve non-contaminated segments.

An example of Power Spectral Density (PSD) for the pure and the filtered EEG signals from both databases are shown in Fig 3.5. Table 3.1 displays Mean±SD of MSE and CC between PSDs of the pure and filtered EEG signals for both simulated databases. As it may be observed, ASWT could preserve EEG components better than methods under comparison.

Fig 3.6 shows PSNR curves as the function of NRMSE for the filtered EEG signals using all methods. As it can be seen, the proposed method gives higher PSNR and lower NRMSE for most of signals than methods under comparison.

Ten seconds fragments of the real and filtered EEG signals resulting from all methods are illustrated in Fig 3.7. Considering that both EEGs and eye blinks were unknown in the original EEG signals, NRMSE, PSNR, and correlation coefficient are not regarded as evaluation criteria of the artifact removal, therefore we have to confine ourselves to visual assessment.

Computational time for the implementation of the algorithm is of great importance for on-line applications. Fig. 3.8 shows the mean±SD of the computational time expressed in seconds for different algorithms and databases per 20 times run.

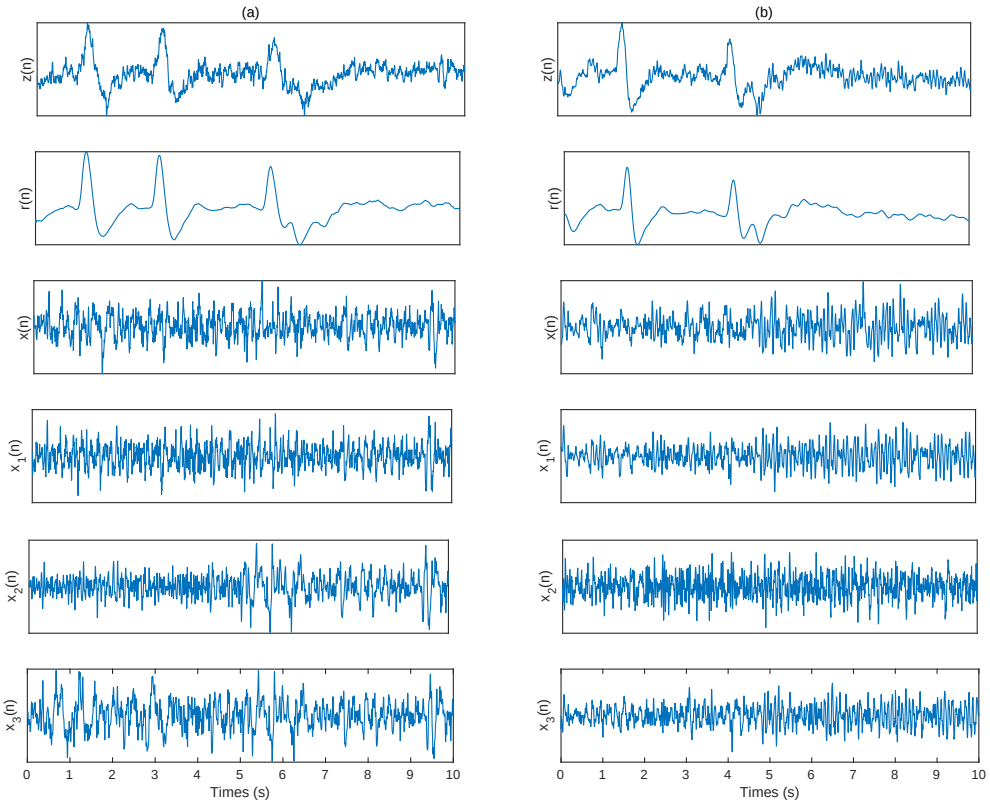

Figure 3.4 Examples of eye blink cancellation in simulated EEG signals from: CHB-MIT (a), and EEG-MAT (b) databases. Each with contaminated EEG $z(n)$, real eye blink artifact $z(n)$, pure EEG $x(n)$, filtered EEG by the proposed method $x_1(n)$, filtered EEG by the AWICA $x_2(n)$ and filtered EEG by the EAWICA $x_3(n)$.

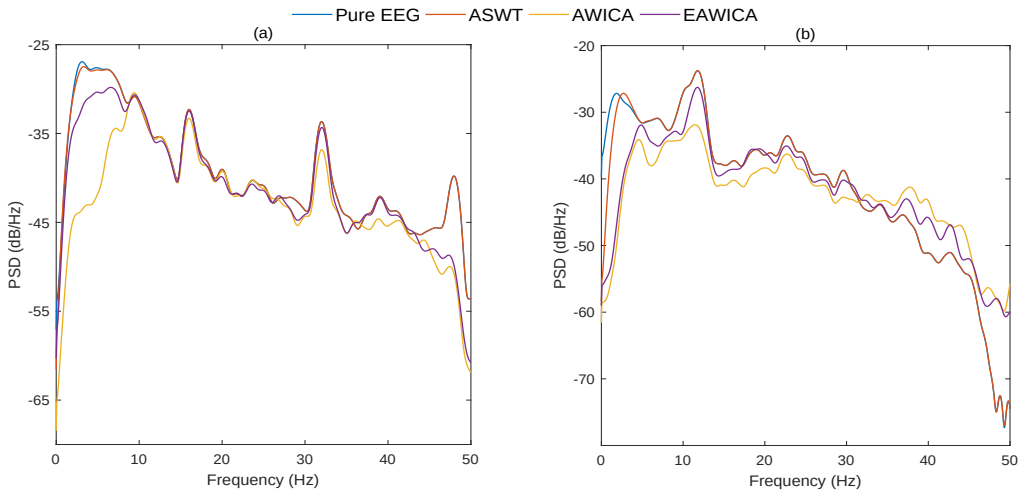

Figure 3.5 Examples of the PSDs for the pure and the filtered EEG signals by all methods for simulated data using CHB-MIT (a) and EEG-MAT (b) databases.

3.2. Results for electrical shift and linear trend elimination

The the mean±SD of NRMSE between the pure and the filtered EEG signals per different values of threshold (T) is shown in Fig 3.9 As it may be seen, the lowest mean NRMSE has been

Table 3.1. Comparison of MSE and CC between the PSDs of the pure and filtered EEG signals for eye blink elimination.

Algorithms	Proposed Method	AWICA	EAWICA
CHB-MIT Database			
MSE	1.76 ± 0.23	3.26 ± 0.56	2.2 ± 0.65
CC	0.85 ± 0.13	0.73 ± 0.21	0.79 ± 0.15
EEG-MAT Database			
MSE	1.96 ± 0.43	4.21 ± 0.74	3.2 ± 0.81
CC	0.83 ± 0.16	0.69 ± 0.28	0.76 ± 0.11

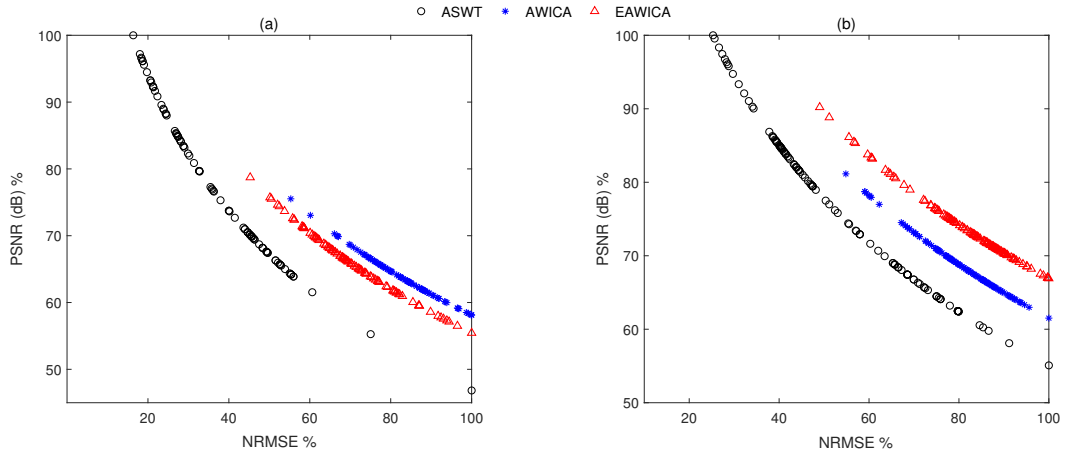

Figure 3.6 PSNR curves as the function of NRMSE for filtered EEG signals CHB-MIT: (a) and EEG-MAT (b) databases. ASWT outperformed the other algorithms because in each subplot, the points associated with the largest PSNR and the smallest NRMSE were achieved by ASWT.

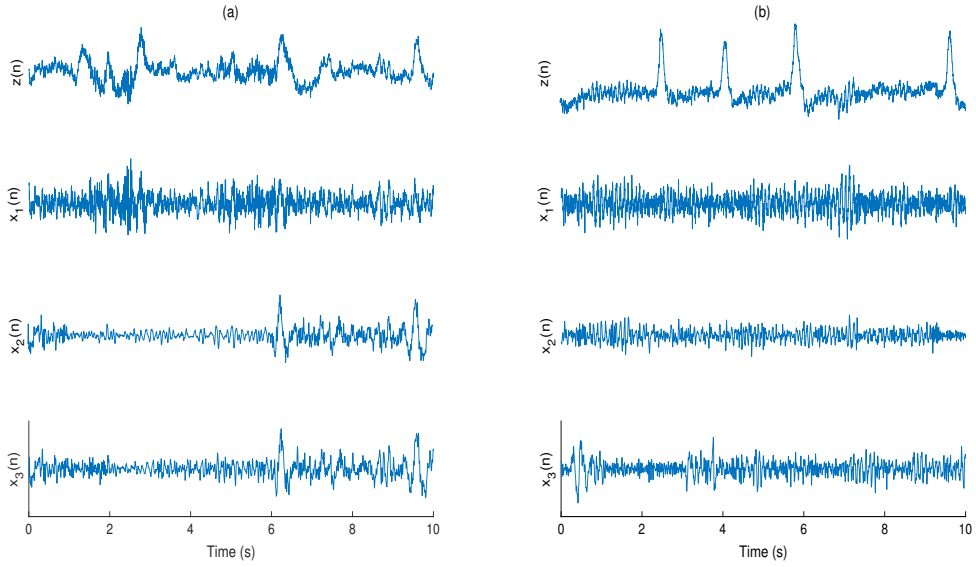

Figure 3.7 Examples of eye blink cancellation in real EEG signals from: BCI Competition 2008 – Graz Data Sets 2a (a), and BCI 2011 left/right motor imagery (b). Each with EEG contaminated with eye blink $z(n)$,filtered EEG by the proposed method $x_1(n)$, filtered EEG by AWICA $x_2(n)$ and filtered EEG by EAWICA $x_3(n)$.

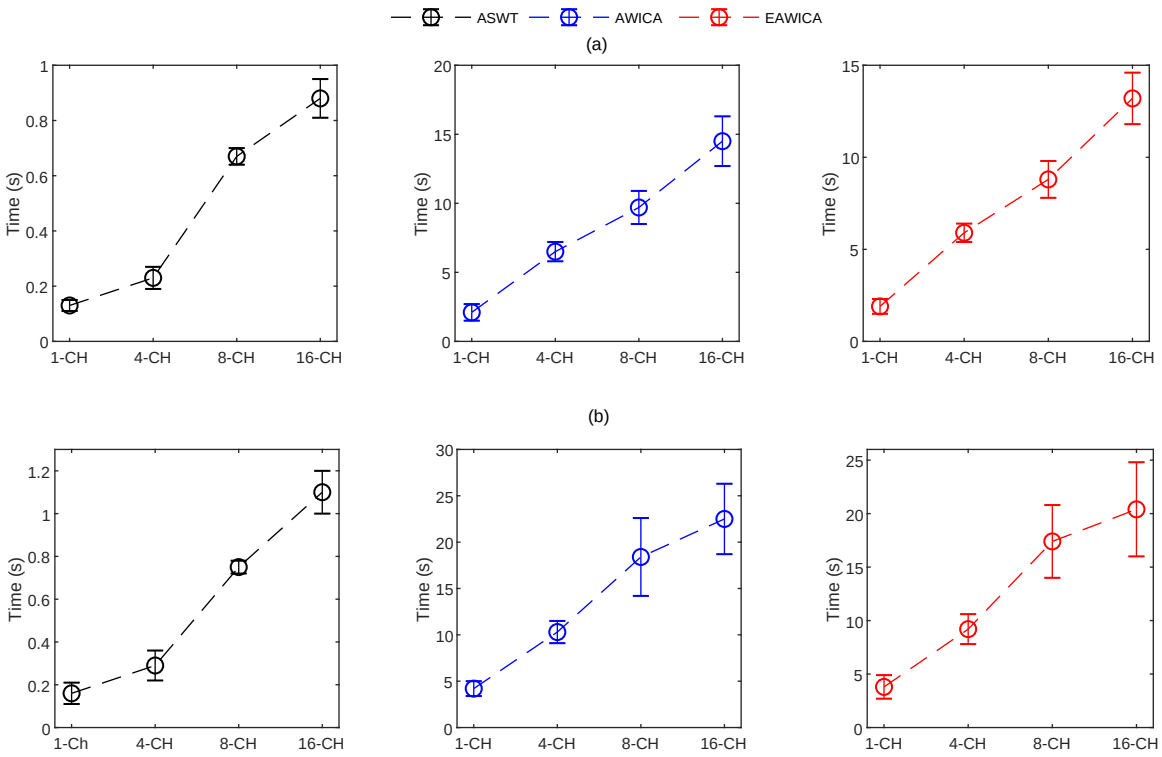

Figure 3.8 The required time for implementation of all algorithms. CHB-MIT (a) and EEG-MAT (b) databases for different EEG channel settings.

achieved by T=0.1. In order to compare the performance of the proposed method with AWICA and

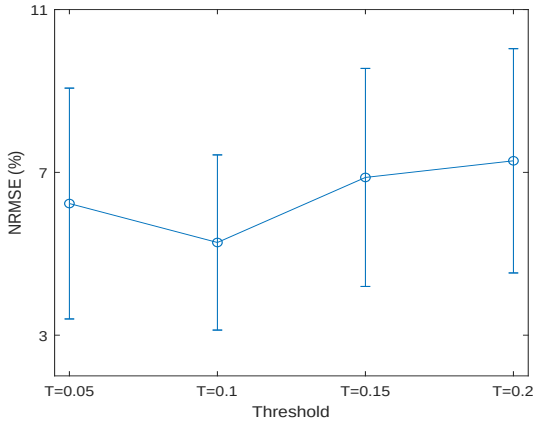

Figure 3.9 Mean±SD of NRMSEs per different T values.

EAWICA, the filtered signals are analyzed in terms of the visual inspection, quantitative metrics and the spectral response. Since the linear trend and electrical shift artifacts in EEG signals are vividly detectable, the performance of all algorithms was visually assessed. Examples of the pure, contaminated and filtered EEG signals using all algorithms are shown in Fig 3.10. As it can be observed, the proposed method performs better in the removal the artifacts components than the methods under comparison; whereas the EEG signals filtered with AWICA and EAWICA still contain some artifacts components.

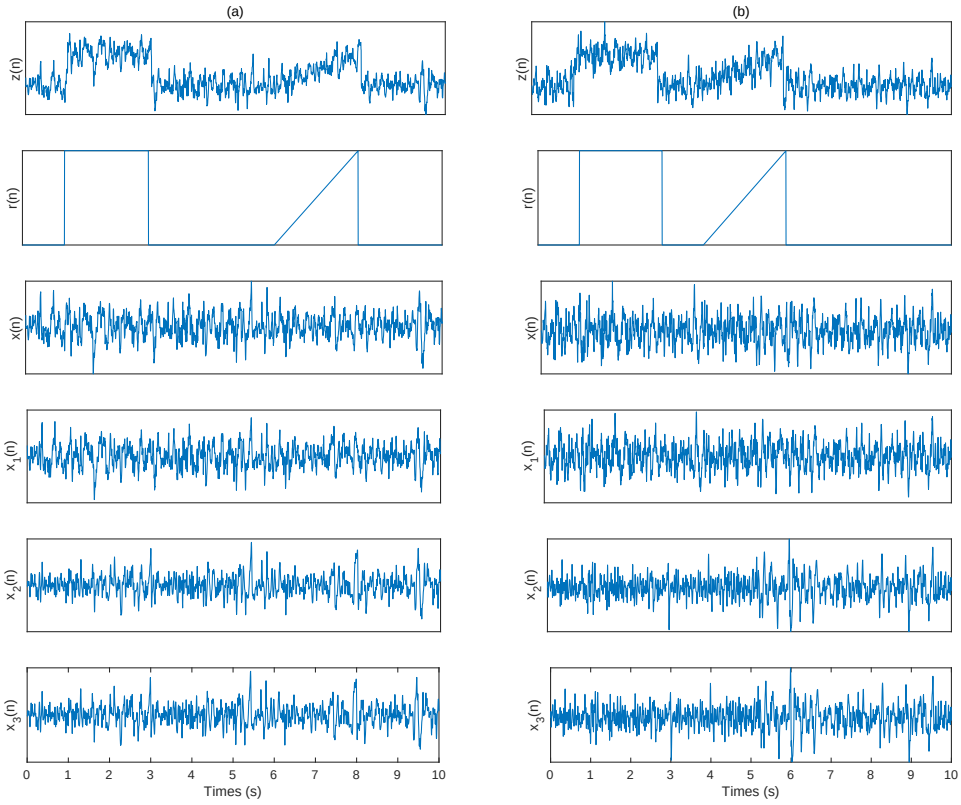

Figure 3.10 Two examples (a) and (b) for visual comparison each with contaminated EEG $z(n)$, pure EEG $x(n)$, filtered EEG by the proposed method $x_1(n)$, filtered EEG by the AWICA $x_2(n)$ and filtered EEG by the EAWICA $x_3(n)$.

NRMSE, PSNR and correlation coefficient are three performance metrics which have been computed for quantitative analysis of this experiment. It should be noted that these metrics were solely computed for the EEG signals contaminated with the simulated artifacts. For the real data, due to lack of the clean EEG data, the performance of the proposed method is evaluated only visually. Fig 3.11 displays the boxplots of the correlation coefficient, NRMSE and PSNR values between the pure and the filtered EEG signals.

The PSNR curves for the reconstructed EEG signals using all algorithms as a function of correlation coefficient are illustrated in Fig 3.12. It is clear that higher PSNR and correlation coefficient have been achieved by the proposed method.

Magnitude Squared Coherence (MSC) and Power Spectral Density (PSD) have been employed to analyze the influence of all algorithms on the frequency components of the filtered EEG signals. The PSD computed with the Welch algorithm and MSC between the pure and the corresponding filtered EEG signals by all methods are shown in Fig 3.13.

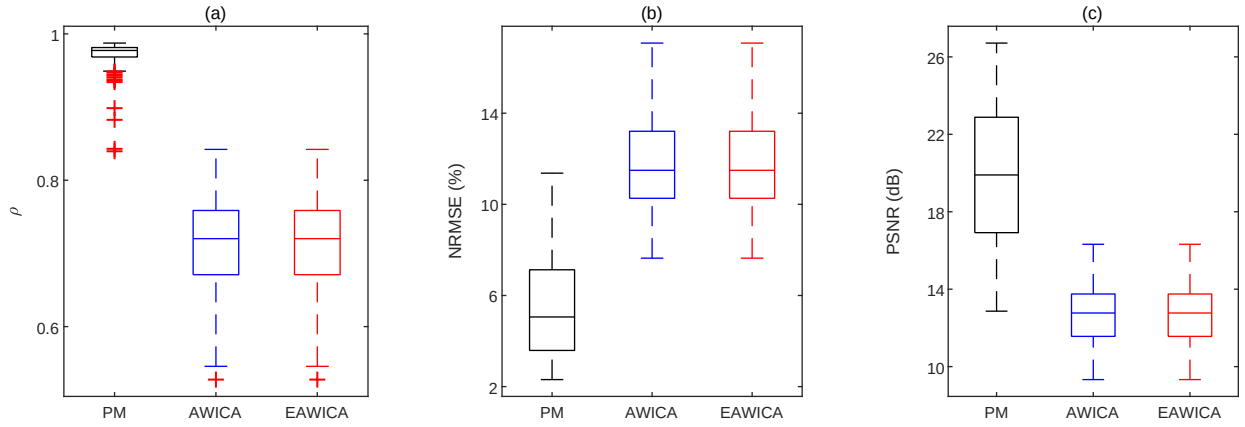

Figure 3.11 Box plots of correlation coefficient (a), NRMSE (b) and PSNR (c) between the pure and filtered EEG for simulated data by all methods. (PM indicates the proposed method).

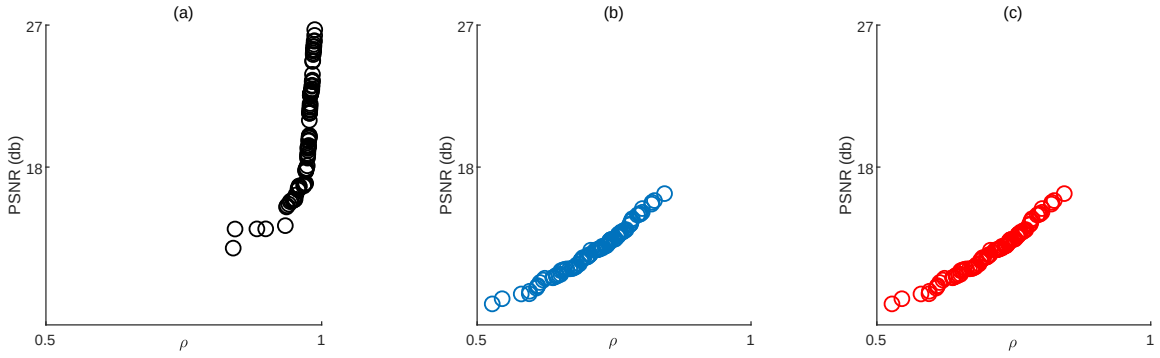

Figure 3.12 The PSNR curves as a the function of correlation coefficient between the pure and the reconstructed EEG signals for the proposed method (a), AWICA (b) and EAWICA (c).

Table 3.2 shows mean±sd of MSE and correlation coefficient for PSDs between the pure and the filtered EEG signals using all algorithms. As it is displayed, the lowest MSE and the highest correlation coefficient have been achieved by the proposed method.

Table 3.2. Comparison of MSE and CC between the PSDs of the pure and filtered EEG signals for ESLT elimination.

Algorithms	Proposed Method	AWICA	EAWICA
MSE	1.66 ± 0.23	3.99 ± 0.67	3.53 ± 0.59
CC	0.87 ± 0.16	0.75 ± 0.38	0.78 ± 0.23

From PSD and MSC point of view, the proposed algorithm better preserved the low frequency components of the EEG signal.

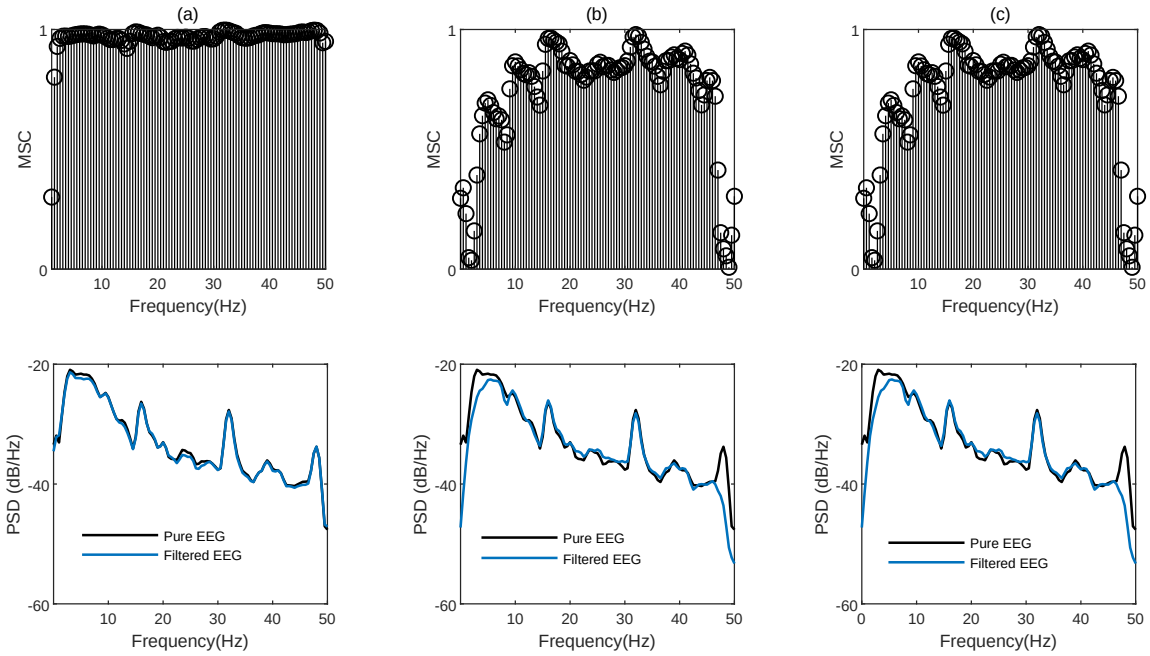

Figure 3.13 An example of MSC and PSD between the pure and filtered EEG signal by the proposed method (a), AWICA (b) and EAWICA (c).

Five-second fragment of the real and filtered EEG signals resulting from the proposed method are illustrated in Fig 3.14. According to the visual assessment of the EEG expert, the proposed method could successfully remove the artifacts components and the result of the filtering is satisfactory.

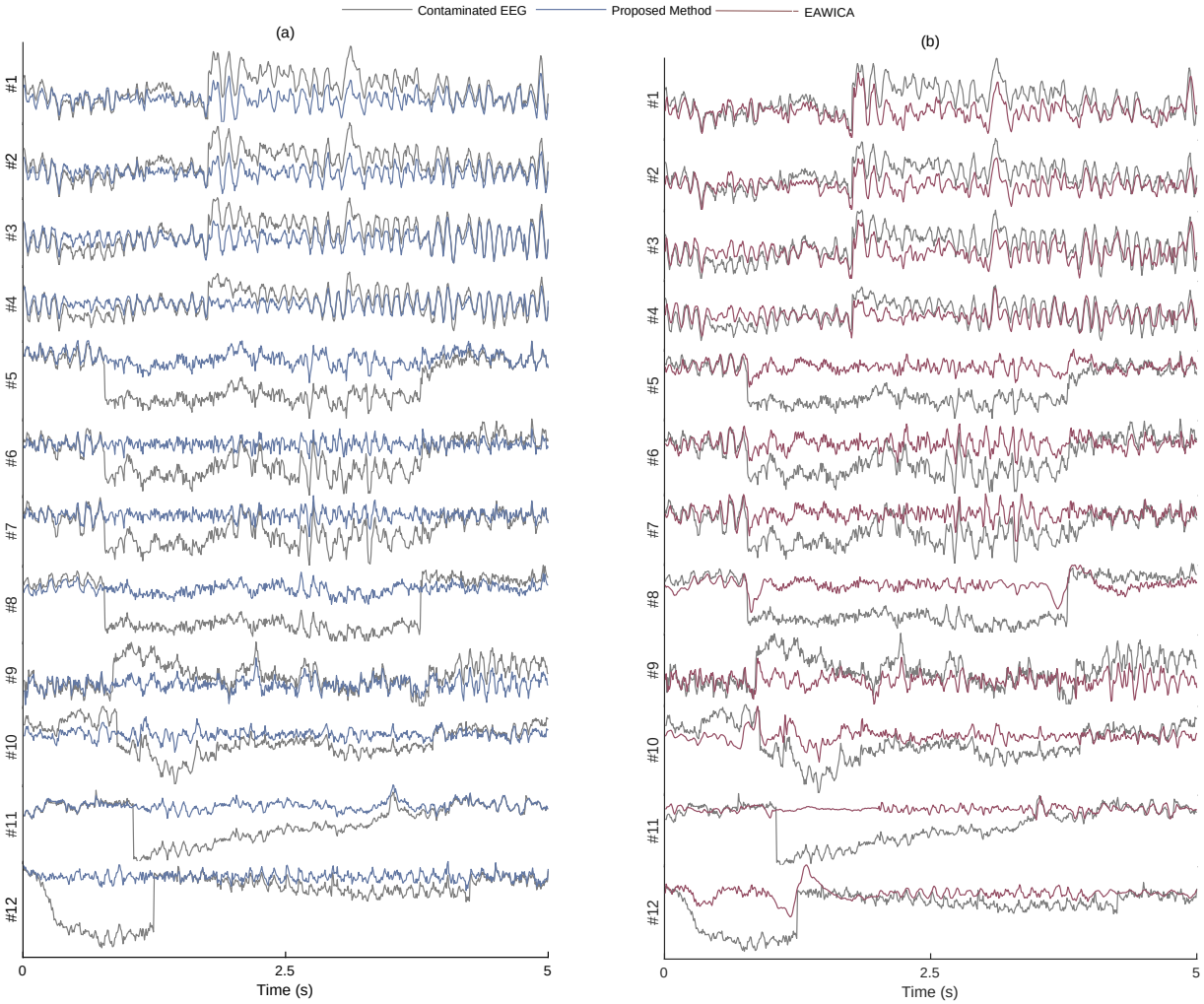

Figure 3.14 Filtering results of real contaminated EEG signals by the proposed SWT-kurtosis (a) and EAWICA (b) algorithms.

Fig. 3.15 shows the required time for denoising CHB-MIT database per different channel settings. As it can seen, the proposed method require much shorter time than algorithms for comparison for all channel settings.

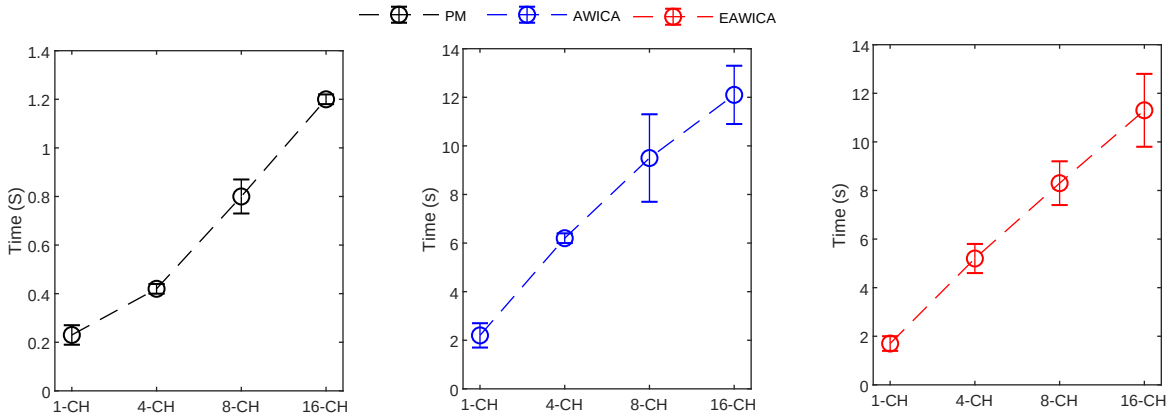

Figure 3.15 The required time for implementation of all algorithms for different EEG channel settings of CHB-MIT database.

4. Discussion

Many approaches for elimination of artifacts from EEG signals have been already described in literature. The main drawbacks of such methods are the necessity of an extra reference channel recording for those based on adaptive filter, the lack of performance of linear filtering when the target signal and artifacts overlap in the same frequency band, the computational expensiveness of BSS methods, and the manual setting of the level of decomposition for source decomposition methods [57].

In this project, we proposed two low-complexity algorithms for elimination of EB an ESLT artifacts from EEG signals. The performance and implementation of the proposed method was compared against AWICA and EAWICA algorithms [17, 42] which were proposed for automatic artifact reduction from EEG signals.

The main motivation behind the selection of SWT over other source decomposition algorithms such as BSS or EMD is its steadiness to decompose EEG signals into several frequency bands with high temporal resolution, which can yield the simpler denoising method as lower computational complexity is required compared to those methods [58]. Moreover, translation-invariance property of SWT compared to DWT is the reason to select SWT over DWT [59].

The objective performance evaluation of the artifact removal techniques is of great importance for a fair justification of the algorithm's effectiveness. It might be influenced by the lack of pure data, insufficient amount of data, casual choice of performance metrics etc. Thus, additionally to the qualitative evaluation such as the time domain plot of the signals or the comparison of PSD between the pure and filtered signals in the spectral domain, reliable quantitative criteria are also required. In order to fulfill this objective, the correlation coefficient, PSNR and NRMSE between the pure and the filtered EEG signals in time domain have been computed. Correlation coefficient was applied to evaluate the degree of linear dependence (phase distortion) between the pure and filtered signals. PSNR was used to compute the peak error of the filtered signals obtained using all algorithms. Indeed, it was applied to calculate the quality of the lossy reconstruction. The higher the PSNR, the better the quality of the reconstructed signal is. NRMSE shows the average difference of the amplitudes between the pure signal and the filtered signal. The smaller NRMSE, the better quality of the filtered signal is.

4.1. Eye blink elimination

The innovation of the method presented for EB elimination in this research resides in combining SWT based decomposition with skewness analysis for automatic selection of a final wavelet decomposition level to extract and subtract eye blink components from the EEG signals. The main assumption for selection of skewness based criteria is a pronounced asymmetry of amplitude values of the EEG signal at the eye blinks dominated episodes.

In total, 216 simulated eye blink contaminated EEG signals from two databases have been processed. Fig. 3.3 shows the box plots of the correlation coefficient and NRMSE between pure and filtered EEG signals of both simulated databases for all algorithms. It can be seen, in most

of the cases, ASWT outperforms the other algorithms. Indeed, in 52 out 216 simulated signals AWICA and EAWICA performed better than ASWT. Examples of visual evaluation of eye blink filtering by all algorithms and corresponding pure EEG signals for both databases are shown in Fig. 3.4. Fig. 3.5 shows the examples of the corresponding PSD for the pure and the filtered EEG signals for both simulated databases. It could be observed that lesser attenuation and distortion of the filtered EEG was achieved by ASWT. Moreover, PSNR curve as the function of NRMSE for both databases are shown in Fig 3.6 (each PSNR was normalized in regard to the highest PSNR value and multiplied by 100) [42]. It is clear that ASWT performed superior for the majority of the simulated data. In order to investigate the performance of the proposed method for real life EEG signals, 16 real eye blink contaminated EEG signals from two databases have been used. Fig. 3.7 demonstrates the examples of the real noisy and filtered EEG signals for both databases. It might be seen that the proposed method could eliminate eye blinks with lower distortion of EEG signals.

Computational complexity is another important factor for the usability of the artifact removal approaches. The comparison of algorithms execution for different databases is shown in Fig 3.8. For a single channel setting of simulated signals from CHB-MIT database with $Fs = 256Hz$ the proposed method was 12x faster than AWICA and 10x faster than EAWICA. As the sampling frequency increases, the algorithms require a longer time to be executed. ASWT was 27x and 25x faster than AWICA and EAWICA, respectively, for a single channel of simulated signals from EEG-MAT database with $Fs = 500Hz$. Additionally, as the length of signals increased for real eye blinks contaminated EEG signals, execution of the AWICA and EAWICA required a considerably longer time than ASWT. The computational time needed for the algorithms for comparison was considerably higher than for the proposed method, thus, they can not be applied for real-time processing.

4.2. Electrical shift and linear trend elimination

The novelty of the proposed method consists of combining SWT based decomposition with kurtosis analysis in order to automate the selection of a final wavelet decomposition level, suitable to detect electrical shift and linear trend artifacts components and then eliminate them from the contaminated EEG signals. The kurtosis has already been introduced as the proper index for the detection of artifact components since artifacts may be typically characterized by the peaky distribution [42].

In total, 96 EEG signals contaminated with simulated electrical shift and linear trend artifacts been applied for the quantitative analysis of difference between all algorithms. Fig. 3.10 shows two examples of the pure, contaminated and filtered EEG signals using all methods. Boxplots of correlation coefficient, NRMSE and PSNR values between the pure and filtered EEG signals for all algorithms are illustrated in Fig. 3.11. The graphs of PSNR as the function of correlation coefficient using all the techniques are shown in Fig. 3.12. Fig. 3.13. shows MSC and PSD between a pure and filtered EEG signals by all techniques. The value of MSC will always fall between 0 to 1. The ideal case is the value of one for all frequencies. As a result, when the value of the MSC is higher, the quality of the filtering is better. According to the obtained results from

Table 3.2, the proposed method performed more effectively for the simulated data.

Fig. 3.14 shows examples of the contaminated and filtered real EEG signals by the proposed method. The obtained results suggests that the proposed method could detect and eliminate epochs contaminated with the artifacts efficiently.

Apart from the performance of the algorithms, another important factor has been considered for the usability of the artifact removal approaches is the computational complexity. The time needed for the proposed method to filter EEG signals were approximately 12 times and 10 times shorter than the AWICA and EAWICA for a single channel setting of EEG (Fig 3.15).

Conclusions and Future work

In this research, two algorithms for the elimination of EB and ESLT artifacts from EEG signals were proposed. The obtained results acknowledge that following objectives have been accomplished:

1. The proposed methods are low-complexity algorithms for filtering of EB and ESLT artifacts, which require neither the artifact reference nor prior knowledge for the recorded EEG signals. In comparison with AWICA and EAWICA algorithms, the required time by the proposed methods for the denoising a single EEG channel is approximately 12 times shorter. Additionally, while the proposed methods only require one parameter to be set before processing, algorithms for comparison require five.

2. The performance of proposed algorithm for the majority of the EB contaminated EEG signals outperformed the algorithms for comparison. Indeed, in 52 out 216 simulated signals, AWICA and EAWICA performed better than the proposed method. In regard to ESLT artifact elimination, the proposed method outperformed the AWICA and EAWICA for all signals. A plausible explanation for this could be because AWICA and EAWICA algorithms erroneously set the artifacts markers, thereby eliminating desirable EEG parts instead of artifacts.

While it requires more investigation, the execution times for the denoising EEG signals with different channel settings show that the proposed algorithms may have a potential to be integrated for portable single-to-few EEG channel systems. It should also be noted that the proposed algorithms were developed on non-epileptic EEG segments. Therefore, the future work of this research is to consider epileptic EEG signals for the denoising.

Appendix

List of Dissemination Activities:

1. M. Shahbakhti, A. Rodrigues, P. Augustyniak, A. Broniec-Wojcik, A. Solosenko, M. Beiramvand, and Vaidotas Marozas, SWT-Kurtosis Based Algorithm for Elimination of Electrical Shift and Linear Trend Artifacts from EEG Signals, Under Review at IEEE Journal of Biomedical and Health Informatics.
2. M. Shahbakhti, M. Maugeon, M. Beiramvand and V. Marozas, Low Complexity Automatic Stationary Wavelet Transform for Elimination of Eye Blinks from EEG , Brain Sci. 2019, 9, 352; doi:10.3390/brainsci9120352

References

[1] R. Flink, B. Pederson, A.B. Guekht, K. Malmgren, R. Michelucci, B. Neville, F. Pinto, U. Stephani and C. Özkara,"Guidelines for the use of EEG methodology in the diagnosis of epilepsy,"*Acta Neurol. Scand*, Vol. 106. p.p. 1–7, 2002.

[2] W.O. Tatum, G. Rubboli, P.W. Kaplan, S.M. Mirsatari, K. Radhakrishnan, D. Gloss, L.O. Caboclo, F.W. Drislane, M. Koutroumanidis, D.L. Schomer, D. Kasteleijn-Nolst Trenite, M. Cook and S. Beniczkym, "Clinical utility of EEG in diagnosing and monitoring epilepsy in adults,"*J. Clin. Neurophysiol*, Vol. 129, p.p. 1056–1082, 2018.

[3] N. Houmani, F. Vialatte, E. Gallego-Jutglà, G. Dreyfus, V.H. Nguyen-Michel, J. Mariani and K, Kinugawa, "Diagnosis of Alzheimer's disease with Electroencephalography in a differential framework,"*Plos One*, Vol. 13, p.p. 1–19, 2018.

[4] S.J.M. Smith,"EEG In Neurological Conditions Other Than Epilepsy: When Does It Help, What Does It Add?,"*J. Neurol. Neurosurg. Psychiatry*, Vol. 76, p.p.8–12, 2005.

[5] Y, Ma, W. Shi, C.K. Peng and A.C. Yang,"Nonlinear dynamical analysis of sleep electroencephalography using fractal and entropy approaches,"*Sleep Med. Rev*. Vol. 37, p.p. 85–93, 2018.

[6] I. Pisarenco, M. Caporro, C. Prosperetti and M. Manconi,"High-density electroencephalography as an innovative tool to explore sleep physiology and sleep related disorders,"*Int. J. Psychophysiol*. Vol. 92, p.p. 8–15, 2014.

[7] R. Abiri, S. Borhani, E.W. Sellers, Y. Jiang and X.A. Zhao,"comprehensive review of EEG-based brain-computer interface paradigms,"*J. Neural Eng*, Vol. 16, p.p. 23-33, 2019.

[8] N. Alharabi,"A Novel approach for noise removal and distinction of EEG recording,"*Biomed. signal process*, Vol. 39, p.p.23-33, 2018.

[9] A. W. Wood, A. Bartel, P. Cadusch, J. Ciorciari, D. Crewther, P. Line, J. Patterson, M. Schier and B. Thompson, "Physiology, Biophysics, and Biomedical Engineering,"*Tayloy and Francis Group*,6000 Broken Sound Parkway NW, 2012.

[10] S. Sanei and J.A. Chambers,"EEG Signal Processing,"*John Wiley and Sons Ltd*,West Sussex PO19 8SQ, England, 2017.

[11] H. Jasper, "Report of the committee on methods of clinical examination in electroencephalography,"*Electroencephalogr Clin Neurophysiol*, Vol. 10 p.p. 370—375, 1985.

[12] P. Berg and M. Scherg,"Dipole modelling of eye activity and its application to the removal of eye artefacts from the EEG and MEG,"*Clin. Physiol. Meas*, Vol. 12, p.p. 49–54, 1991.

[13] A. Crespel, P. Gélisse, M. Bureau and P. Genton,"In Atlas of Electroencephalography,"*J. Libbey Eurotext*, 2005.

[14] R. Guarnieri, M. Marino, F. Barban, M. Ganzetti and D. Mantini, "Online EEG artifact removal for BCI applications by adaptive spatial filtering," *J. Neural Eng.*, vol. 15, pp. 1–12, 2018.

[15] S. Blum, N. S. J. Jacobsen, M. G. Bleichner and S. Debener, "A Riemannian Modification of Artifact Subspace Reconstruction for EEG Artifact Handling," *FRONT HUM NEUROSCI*, vol. 13, pp. 1–10, 2019.

[16] N. Bajaj, J. R. Carrión, F. Bellotti, R. Berta, A. D. Gloria, "Automatic and tunable algorithm for EEG artifact removal using wavelet decomposition with applications in predictive modeling during auditory tasks," *Biomed Signal Process Control*, Vol. 55, pp. 1–13, 2020.

[17] N. Mammone, F. L. Foresta and F. C. Morabito, "Automatic Artifact Rejection From Multichannel Scalp EEG by Wavelet ICA," *IEEE Sens. J.*, vol. 12, no. 3, pp. 533–542, 2012.

[18] B. K. Giri, S. Sarkar, S. Mazumder and K. Das, "A Computationally Efficient Order Statistics based Outlier Detection Technique for EEG Signals," in *Conf Proc IEEE Eng Med Biol Soc*, Milan, 2015, pp. 4765–4768.

[19] S.C Ng and P. Raveendran, "Enhanced μ Rhythm Extraction Using Blind Source Separation and Wavelet Transform,"*IEEE Trans. Biomed. Eng*, Vol. 56, p.p. 2024–2034, 2009.

[20] C. Porcaro, M.T. Medaglia and A. Krott,"Removing speech artifacts from electroencephalographic recordings during overt picture naming,"*Neuroimage*, Vol. 105, p.p. 171–180, 2015.

[21] C. Porcaro, J.H. Balsters, D. Mantini, I.H. Robertson and N. Wenderoth,"P3b amplitude as a signature of cognitive decline in the older population: An EEG study enhanced by Functional Source Separation,"*Neuroimage*, Vol. 184, p.p. 533–546, 2019.

[22] P. He, G. Wilson and C. Russell,"Removal of ocular artifacts from electro-encephalogram by adaptive filtering,"*Med. Biol. Eng. Comput*,Vol. 42. p.p. 407-412, 2004.

[23] S. Weisdorf, J. Duun-Henriksen, M.J. Kjeldsen, F.R. Poulsen, S.W. Gangstad and T.W. Kjaer,"Ultra-long-term subcutaneous home monitoring of epilepsy-490 days of EEG from nine patients,"*Epilepsia*, 2019.

[24] J.W. Ahn, Y. Ku and H.C. Kim,"A Novel Wearable EEG and ECG Recording System for Stress Assessment,"*Sensors*, Vol. 19, 2019.

[25] M. Izzetoglu, A. Devaraj, S. Bunce and B. Onaral,"Motion artifact cancellation in NIR spectroscopy using Wiener filtering,"*IEEE Trans. Biomed. Eng*, Vol. 52, p.p. 934–938, 2005.

[26] A. Borowicz,"Using a multichannel Wiener filter to remove eye-blink artifacts from EEG data,"*Biomed Signal Process Control*, Vol. 45, p.p. 246-255, 2018.

[27] C.J. James and C.W. Hesse,"Independent component analysis for biomedical signals,"*Physiol Meas*, Vol. 26, p.p. 15-39, 2005.

[28] S. Fitzgibbon, D. Powers, K. Pope and C. Clark, "Removal of EEG noise and artifact using blind source separation,"*J Clin Neurophysiol*, Vol. 24, p.p. 232-243, 2007.

[29] T. Lagerlund, F. Sharbrough and N. Busacker, "Spatial filtering of multichannel electroencephalographic recordings through principal component analysis by singular value decomposition,"*J Clin Neurophysiol*, Vol. 14, p.p. 73-82, 1997.

[30] M. K. I. Molla, T. Tanaka, T. M. Rutkowski and A. Cichocki, "Separation of EOG artifacts from EEG signals using bivariate EMD,"*In Proceedings of the IEEE International Conference on Acoustics, Speech, and Signal Processing (ICASSP)*, Dallas, TX, USA, pp. 562–565, 2010.

[31] D. Safieddine, A. Kachenoura, L. Albera, G. Birot, A. Karfoul, A. Pasnicu, A. Biraben, F. Wendling, L. Senhadji and I. Merlet,"Removal of muscle artifact from EEG data: Comparison between stochastic (ICA and CCA) and deterministic (EMD and wavelet-based) approaches,"*EURASIP J. Adv. Signal Process*, Vol. 127, 2012.

[32] C. Dora and P. K. Biswal,"An improved algorithm for efficient ocular artifact suppression from frontal EEG electrodes using VMD,"*Biocybern. Biomed. Eng.*, Vol. 40, No.1, 2019.

[33] C. Dora and P. K. Biswal,"Correlation-based ECG Artifact Correction from Single Channel EEG using Modified Variational Mode Decomposition,"*Comput Methods Programs Biomed*, Vol. 183, 2020.

[34] E. Estrada, H. Nazeran, G. Sierra, F. Ebrahimi and S. K. Setarehdan, "Wavelet-based EEG de-noising for automatic sleep stage lassification,"*In Proceedings of the 21st International Conference on Electronics, Communications, and Computers.*, Cholula, Mexico,pp. 295–298, 2011.

[35] J. Gao, H. Sultan, J. Hu and W. Tung, "Denoising nonlinear time series by adaptive filtering and wavelet shrinkage: A comparison,"*IEEE Signal Proc. Lett*, Vol. 17, p.p. 237-240, 2010.

[36] P. Chrapka, H. Bruin, G. Hasey and J. Reilly,"Wavelet-Based Muscle Artefact Noise Reduction for Short Latency rTMS Evoked Potentials,"*IEEE Trans Neural Syst Rehabil Eng*, Vol. 27, No. 7, p.p. 1449-1457, 2019.

[37] P. Gajbhiye, R. K. Tripathy, A. Bhattacharyya and R. B. Pachori,"Novel Approaches for the Removal of Motion Artifact From EEG Recordings,"*IEEE SENS J*, Vol. 19, No. 22, p.p. 10600 - 10608, 2019.

[38] N. E. Huang, Z. Shen, S. R. Long, M. C. Wu, H. H. Shih, Q. Zheng, N. C. Yen, C. C. Tung and H. H. Liu,"The Empirical Mode Decomposition and the Hilbert Spectrum for Nonlinear and Nonstationary Time Series Analysis,"*Proceedings of the Royal Society of London A.* Vol. 454, p.p. 903–995, 1998.

[39] Z. Wu and N. E. Huang,"Ensemble Empirical Mode Decomposition: A Noise-Assisted Data Analysis Method,"*Adv. Adapt. Data Anal.*, Vol. 1, p.p. 1-41, 2009.

[40] T. Zikov, S. Bibian, G. Dumont, M. Huzmezan, and C. Ries,"A wavelet based de noising technique for ocular artifact correction of the electroencephalogram,"*in Proc. Second Joint EMBS/BMES Conf.*, pp. 98–105, 2002.

[41] R. Brychta, S. Tuntrakool, M. Appalsamy, N. Keller, D. Robertson, R. Shiavi, and A. Diedrich,"A Wavelet methods for spike detection in mouse renal sympathetic nerve activity,"*IEEE Trans. Biomed. Eng.*, vol. 54, pp. 82–93, 2007.

[42] N. Mammone and F. C. Morabito, "Enhanced Automatic Wavelet Independent Component Analysis for Electroencephalographic Artifact Removal,"*Entropy*, vol. 16, pp. 6553–6572, 2014.

[43] H. Ghandeharion and A. Erfanian, "A fully automatic ocular artifact suppression from EEG data using higher order statistics: Improved performance by wavelet analysis,"*MED ENG PHYS*, vol. 32, No. 7, pp. 720–729, 2020.

[44] M. F. Issa and Z. Juhasz, "Improved EOG Artifact Removal Using Wavelet Enhanced Independent Component Analysis,"*Brain Sci*, vol. 9, No. 12, pp. 1–22, 2019.

[45] R. Patel, P.R. Madhukar Janawadkar, S. Sengottuvel, K. Gireesan and T.S. Radhakrishnan,"Suppression of Eye-Blink Associated Artifact Using Single Channel EEG Data by Combining Cross-Correlation with Empirical Mode Decomposition,"*IEEE Sens. J.*, Vol. 2016, p.p. 6947–6954, 2016.

[46] J. Dammers, M. Schiek, F. Boers, C. Silex, M. Zvyagintsev, U. Pietrzyk and K. Mathiak,"Integration of Amplitude and Phase Statistics for Complete Artifact Removal in Independent Components of Neuromagnetic Recordings,"*IEEE Trans Biomed Eng*, Vol. 5, p.p. 2353–2362, 2008.

[47] S. Javidi, D. P. Mandic, C. C. Took and A. Cichocki, "Kurtosis-based blind source extraction of complex non-circular signals with application in EEG artifact removal in real-time," *Front. Neurosci.*, vol. 5, pp. 1–18, 2011.

[48] R. Mahajan and B.I. Morshed "Unsupervised Eye Blink Artifact Denoising of EEG Data with Modified Multiscale Sample Entropy, Kurtosis, and Wavelet-ICA," *IEEE J BIOMED HEALTH*, vol. 19, pp. 158–165, 2015.

[49] A. Delorme, T. Sejnowski and S. Makei, "Enhanced detection of artifacts in EEG data using higher-order statistics and independent component analysis," *NeuroImage*, vol. 34, pp. 1443–1449, 2007.

[50] N. Bajaj, J. R. Carrión, F. Bellotti, R. Berta and A. D. Gloria,"Automatic and tunable algorithm for EEG artifact removal using wavelet decomposition with applications in predictive modeling during auditory tasks," *Biomed Signal Process Control*, Vol. 55, pp. 1–13, 2020.

[51] A.K. Maddirala and R.A. Shaik,"Removal of EOG Artifacts from Single Channel EEG Signals Using Combined Singular Spectrum Analysis and Adaptive Noise Canceler,"*IEEE Sens. J.*, Vol. 16, p.p. 8279–8287, 2016.

[52] A. Shoeb, "Application of Machine Learning to Epileptic Seizure Onset Detection and Treatment,", PhD Thesis, Massachusetts Institute of Technology, USA, 2009.

[53] I. Zyma, S. Tukaev, I. Seleznov, K. Kiyono, A. Popov, M. Chernykh and O. Shpenkov,"Electroencephalograms during Mental Arithmetic Task Performance,"*Data*, Vol. 4, 2019.

[54] H. Cho, M. Ahn, S. Ahn, M. Kwon and S.C. Jun,"EEG datasets for motor imagery brain-computer interface,"*GigaScience*, Vol. 6, p.p. 1–8, 2017.

[55] B. Blankertz, G. Dornhege, M. Krauledat, k.R. Müller and G. Curio,"The noninvasive Berlin Brain-Computer Interface: Fast acquisition of effective performance in untrained subjects,"*NeuroImage*, Vol. 39, p.p. 539–550, 2007.

[56] A. Delorme and S. Makeig, "EEGLAB: an open source toolbox for analysis of single-trial EEG dynamics including independent component analysis," *J. Neurosci. Methods*, vol.134, pp. 9–21, 2004. Available:(http://sccn.ucsd.edu/eeglab/)

[57] X. Jiang, G. Bian and Z. Tian, "Removal of Artifacts from EEG Signals: A Review,"*SENS*, Vol. 19, No. 987, p.p. 1-18, 2019.

[58] S. Mallat, “A Wavelet Tour of Signal Processing,” *Third Edition: The Sparse Way*, 3rd ed. New York, NY, USA: Academic, 2008.

[59] H. Guo and C. Burrus,“Convolution using the undecimated discrete wavelet transform, ” *in Proc. IEEE Int. Conf. Acoust., Speech, Signal Process*, 1996, vol. 3, pp. 1291–1294.